NASA/CR—2019–220061

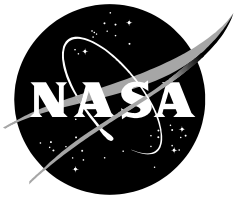

Concept Evaluation: NASA Reference Model 2—Side by Side

Lauren N. Wagner
Kentucky Space Grant Consortium
Ames Research Center, Moffett Field, California

February 2019

NASA STI Program ... in Profile

Since its founding, NASA has been dedicated to the advancement of aeronautics and space science. The NASA scientific and technical information (STI) program plays a key part in helping NASA maintain this important role.

The NASA STI program operates under the auspices of the Agency Chief Information Officer. It collects, organizes, provides for archiving, and disseminates NASA's STI. The NASA STI program provides access to the NTRS Registered and its public interface, the NASA Technical Reports Server, thus providing one of the largest collections of aeronautical and space science STI in the world. Results are published in both non-NASA channels and by NASA in the NASA STI Report Series, which includes the following report types:

- TECHNICAL PUBLICATION. Reports of completed research or a major significant phase of research that present the results of NASA Programs and include extensive data or theoretical analysis. Includes compilations of significant scientific and technical data and information deemed to be of continuing reference value. NASA counterpart of peer-reviewed formal professional papers but has less stringent limitations on manuscript length and extent of graphic presentations.

- TECHNICAL MEMORANDUM. Scientific and technical findings that are preliminary or of specialized interest, e.g., quick release reports, working papers, and bibliographies that contain minimal annotation. Does not contain extensive analysis.

- CONTRACTOR REPORT. Scientific and technical findings by NASA-sponsored contractors and grantees.

- CONFERENCE PUBLICATION. Collected papers from scientific and technical conferences, symposia, seminars, or other meetings sponsored or co-sponsored by NASA.

- SPECIAL PUBLICATION. Scientific, technical, or historical information from NASA programs, projects, and missions, often concerned with subjects having substantial public interest.

- TECHNICAL TRANSLATION. English-language translations of foreign scientific and technical material pertinent to NASA's mission.

Specialized services also include organizing and publishing research results, distributing specialized research announcements and feeds, providing information desk and personal search support, and enabling data exchange services.

For more information about the NASA STI program, see the following:

- Access the NASA STI program home page at http://www.sti.nasa.gov

- E-mail your question to help@sti.nasa.gov

- Phone the NASA STI Information Desk at 757-864-9658

- Write to:
  NASA STI Information Desk
  Mail Stop 148
  NASA Langley Research Center
  Hampton, VA 23681-2199

NASA/CR—2019–220061

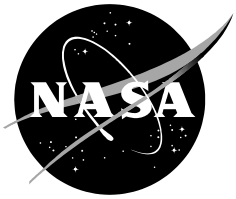

Concept Evaluation: NASA Reference Model 2—Side by Side

Lauren N. Wagner
Kentucky Space Grant Consortium
Ames Research Center, Moffett Field, California

National Aeronautics and
Space Administration

Ames Research Center
Moffett Field, CA 94035-1000

February 2019

ACKNOWLEDGMENTS

First acknowledgements must go to Witold Koning, who has tirelessly supported this project and answered my many questions. His knowledge of RotCFD and its issues made this project possible. His constant good attitude and intelligence are something to be admired.

Chris Silva also deserves recognition for designing the model and providing important details necessary for these simulations. His previous work set the foundation for this project.

Additional thanks goes to the rest of the Simulations Group: Carly Foss, Bonny Allu, Brandon Tieu, Jacob Kowalski, Jason Cornelius, Ali Fares, Curtis Moffett, and Curtis Zicker. Special recognition goes to my office mates in The Cube, Daniel Varner and Mireille Fehler, who made every day in the office enjoyable. Even more special recognition goes to my fellow group lead, Keiko Nagami.

Thanks to William Warmbrodt for helping me get back to this amazing place for a second year. His wisdom and guidance is something I will remember for all time. And finally, recognition also goes to Kentucky Space Grant for funding this adventure.

TABLE OF CONTENTS

LIST OF FIGURES

LIST OF TABLES

NOMENCLATURE

AOA	angle of attack
CAD	computer aided design
CFD	computational fluid dynamics
DGW	design gross weight (lb)
FF	forward flight
GUI	graphical user interface
IGE	in ground effect
NR-2	NASA Reference Model 2
OGE	out of ground effect
OpenVSP	Open Vehicle Sketch Pad
RotCFD	Rotorcraft Computational Fluid Dynamics
UAM	urban air mobility
URANS	Unsteady Reynolds Averaged Navier Stokes
VTOL	vertical takeoff and landing

Concept Evaluation: NASA Reference Model 2—Side by Side

Lauren Wagner[*]

Ames Research Center

SUMMARY

Urban Air Mobility (UAM) is an up and coming topic in the world of aeroscience. A variety of companies, most notably Uber, have begun working towards making air taxis a regular part of day-to-day life. However, the implementation of this system into society will require a significant amount of work: making helicopters that can handle these flights and operate safely in urban environments, having landing zones, and working out new technologies to lower costs. NASA has also taken interest in this new idea and has formed a focus group of interns to tackle some of these problems. They have started by designing a few concept models for these air taxis, focusing on low noise, multiple passenger configurations, and the potential for electric or hybrid helicopters.

One particular model is NASA Reference Model 2, known as NR-2 or the "Side by Side," which features two rotors spinning in opposite directions. Although this model is purely conceptual at this point, understanding the real-world aerodynamics and performance of this model is crucial to its future development. Using a program called Rotorcraft Computational Fluid Dynamics (RotCFD), the performance characteristics of the rotors and aircraft, such as the lift, drag, thrust, and power, can be determined. These simulations can be run in a variety of flight configurations, with hover, forward flight, and climb being focused on in this study. The rotor collective angle can also be changed and used to get results about the lift and drag for the blades and the model body. These simulations can provide information for future model construction and wind tunnel testing.

INTRODUCTION

As cities become more and more populated, the need for improved transportation methods has greatly increased. While many companies have worked to improve ground transportation, including trains, driverless cars, and ridesharing, some companies have begun to look to the sky. As the ground becomes more crowded, and electric aircraft become more feasible, the possibility for short-distance air travel increases. Implementing a system of air travel, commonly referred to as Urban Air Mobility (UAM), will require a great deal of work; massive overhaul in infrastructure, regulations, and innovation will be needed.

One branch of UAM is aircraft development. For crowded cities, designing vertical takeoff and landing (VTOL) aircraft that are quiet, efficient, and easy to fly is a key part of UAM success. Current helicopters and aircraft require large areas to take off and are noisy, making them hard to implement into a city setting. Thus, a new breed of VTOL aircraft is needed, specifically designed for these capabilities.

[*] NASA Kentucky Space Grant Consortium, Lexington, KY 40506-0108.

A variety of companies have taken an interest in designing aircraft specifically for this new field. Companies such as Uber and Kitty Hawk are leading the movement, with models such as BlackFly already available. Many other companies, including NASA, are also creating a variety of conceptual models. However, in the modern era of aircraft design, computer simulation and testing are used to prove the functionality of models before they are built. Simulations allow for a variety of flight conditions and scenarios to be tested, and are much more inexpensive than modeling and physical testing. Thus, in order to fully understand the workings of NASA's conceptual vehicles, several interns have been simulating conceptual models to determine various flight characteristics.

APPROACH

Objectives

The goal of this project is to determine the flight characteristics of NASA Reference Model 2 (NR-2). This model is a six-passenger, two-rotor VTOL, nicknamed the "Side by Side" (Fig. 1). This model meets many of the requirements for UAM, including low noise and varied passenger size, and features a hybrid engine. A variety of conditions were chosen for simulation: hover, forward flight at 0, 4, 6, 8, and 12 degrees, and takeoff out of ground effect (OGE). The helicopter was simulated with accurate propellers in all of these conditions and results were recorded. The main factors noted were thrust, power, lift, and drag. Using these numbers and knowing the design gross weight (DGW) and performance for the aircraft, performance calculations could be derived for the model. These results were compared with other conceptual model figures, and performance differences were noted.

Figure 1. NASA Reference Model 2—Side by Side.

Software

In order to meet the objectives of this project, a program called Rotorcraft Computational Fluid Dynamics (RotCFD) was used to simulate NR-2. RotCFD is a mid-fidelity CFD program, specially designed for rotorcraft. The program is capable of examining rotor performance, blade performance, and body forces. The graphical user interface (GUI) is easy to learn and provides a variety of useful features and post-processing actions. Flow visualization was used heavily throughout this project, as it shows the wake generated by the rotor. Bodies can be imported into the program in order to read body forces. However, the program can only read the force of the full body, so taking the model into another computer aided design (CAD) program and dividing the model can allow for force readings at multiple points. RotCFD rotor generation allows for airfoil tables to be imported, as well as characterizing twist, thickness-to-chord ratios, and hub size.

For this project, the program RotUNS was used to study the VTOL performance. RotUNS utilizes Unsteady Reynolds Averaged Navier Stokes (URANS) equations to make a variety of flow and force calculations. RotCFD version 401 was used, as it does not have a compressible solver, making this a more idealized, but easier to solve, case. RotCFD solves the incompressible, steady equations in its calculations:

Mass Conservation: $\partial\rho/\partial t + \nabla \cdot (\rho V) = 0$

Momentum Conservation: $\partial/\partial t\ (\rho_{ui}) + \nabla \cdot (\rho V_{ui} - \mu\nabla_{ui}) = -\partial p/\partial X_i + V_i + S'_i$

Calculations are performed within each of the cells that are generated within a certain boundary region around the body. Cells can be formed around bodies using the “Fit Bodies” feature, which creates tetrahedral cells around surfaces. Other cells in the program should ideally be square. The time grid in the program is also important, especially when considering rotors. The solver follows a turbulent k-epsilon method.

Model Specifications

In the creation of NR-2, several specifications were given for the model. The model was generated in OpenVSP, and exported as Lithography (*.stl) (Figs. 2–4). In addition to the specifications of a hybrid electric engine, the ability to seat six passengers, and have two rotors, several technical aspects were listed (see Table 1). The values given are theoretical characteristics generated by a program called CAMRAD II, an aeromechanical analysis of helicopters and rotorcraft. Some of the characteristics can be inserted into RotCFD for simulation, while others serve as a comparison point to confirm the accuracy of the simulation. Some of the complexities of the model, including the landing gear and rotor hub, were removed from the model. The simplified NR-2 was then imported into RotCFD, and the sizing was confirmed.

Specifications for the rotor were also provided (see Table 2). Two different airfoil tables were used for the general shape of the rotor, and details about twist and chord-to-thickness ratio were also given. These characteristics were input into RotCFD to generate accurate rotors. When inputting into RotCFD, any break in the r/R can be interpreted as a linear interpolation between the points. With all of these details, the model could be accurately simulated. The rotors could be visually compared in order to confirm accuracy. The left rotor was assumed to spin counterclockwise, and the right rotor clockwise.

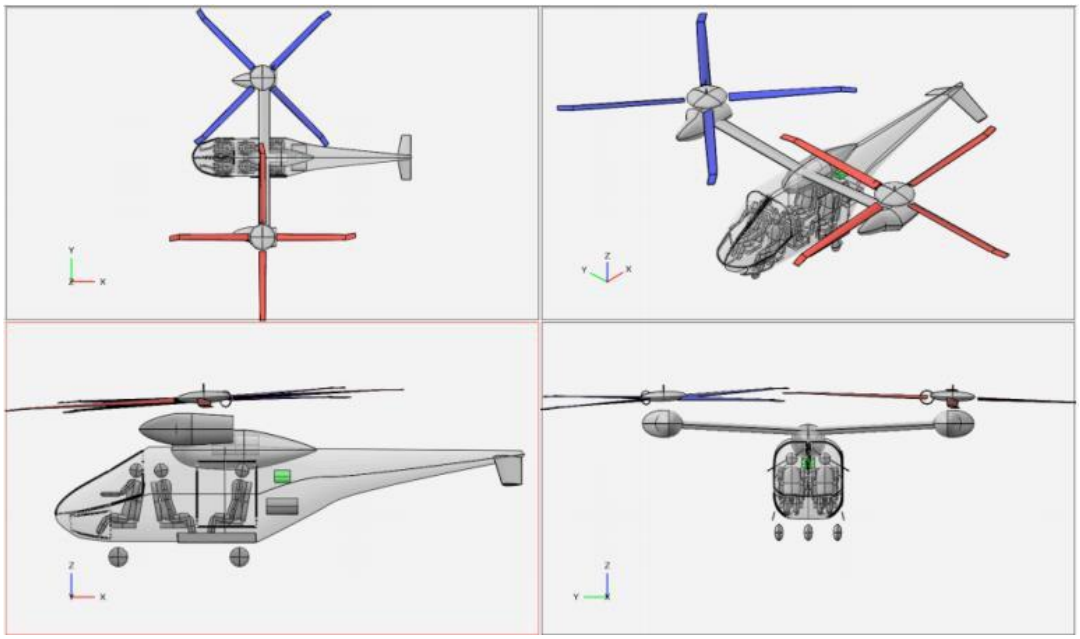

Figure 2. NR-2 arrangements.

Table 1. Design Specifications

Tip Speed (ft/s)	550
Rotor Radius (ft)	11.82
Number of Blades	4
Cruise Speed (knots)	115
Design Gross Weight (lb)	3950
Range (nm)	200
Aircraft FM	0.69

Table 2. Rotor Specifications

Airfoils	**r/R**
Rotor Cutout	0–0.16
soamain	0.16–0.85
soatip	0.95–1.0
Twist (degrees)	
0	0.16
–12	1.0
Thickness to Chord (c/R)	
0.0623	0.16
0.0623	0.85
0.0623	0.94
0.0374	1.0

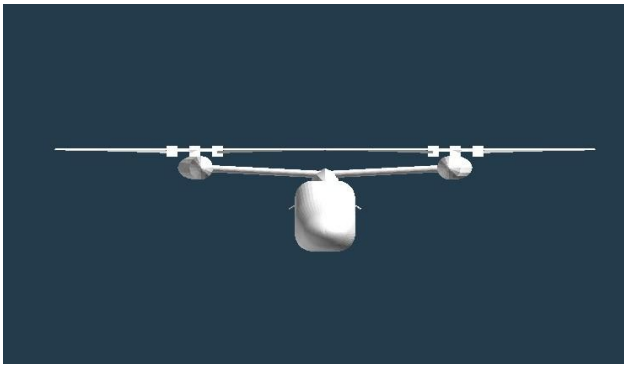

Figure 3. NR-2 RotCFD model—front view.

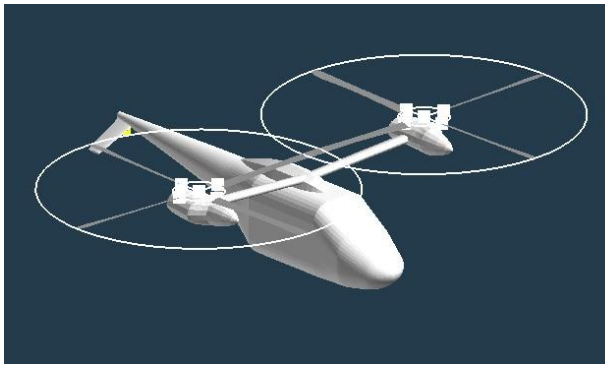

Figure 4. NR-2 RotCFD model—isometric.

Initial simulations also led to other rotor inputs being changed. The default pitch angle of 10 degrees did not provide enough thrust to lift the body; therefore the pitch was adjusted to 20 degrees, which more than compensated for weight. This is higher than desirable for a collective pitch, but since the rotors are not finalized this can be somewhat overlooked. This was also not a refined selection of pitch, but an estimation of roughly what pitch would produce enough lift. Since no pitch angle was provided in the initial report about NR-2, 20 degrees was a fair assumption. The rotors were also run in steady state, which treats the rotor like a constant disk, but also runs simulations with less restrictions, therefore making it quicker.

Setup

1. General Setup

A variety of settings can be put into RotCFD, including flow conditions, wall properties, positioning, and analysis methods. Some of these are consistent across all cases, while others were changed depending on the flight configuration. Consistency in some setups allows for more accurate comparison of results. Other than flight conditions, walls, and time grid, all other settings were kept the same. All inputs are in English units. An in ground effect (IGE) case utilized a different gridding in order to place the model 1.5 rotors above a viscous wall.

The flow properties for all normal cases were run around sea level (see Table 3). Even though the cruise height at sea level is around 5,000 feet, short flights are unlikely to reach this height. Additionally, this altitude change barely affects the flow properties. One special case was run in order to compare the two points.

Table 3. Flow Properties

Flow Properties	Value
Static Density (lb/ft^3)	2.38E-3
Static Temperature (R)	518.69
Gas Constant	1716.48
Dynamic Viscosity ($lb\ s/ft^2$)	3.7384E-7
Static Pressure (lb/ft^2)	2116.2

Setting realistic boundary conditions is another important aspect of simulations (see Table 4). One rule for setting boundary conditions is the 5-5-10 rule. This rule is based on rotor diameter, and sets the boundaries at 5 diameters above, 5 diameters around, and 10 diameters below the rotor. The radius of this rotor is approximately 12 feet, which gives a diameter of 24 feet. Refinement and cell count were set to keep gridding level changes from being too drastic, while also maintaining a square cell shape. Square cells ensure equal calculations, no matter where the flow is coming from.

In order to accurately read the forces happening at different parts of the body, NR-2 was split into several parts (Fig. 5). In addition to the two separate rotors, the main helicopter body was divided into three parts (Fig. 6): 1. fuselage, 2. wing with nacelles, and 3. tail. The forces can be read on each of these sections, in all directions. Total force is also calculated.

Table 4. Boundary Setup

Boundary	Position	Refinement	Cell Count
X-Min	–120	3	8
X-Max	–120	3	
Y-Min	–240	3	8
Y-Max	120	3	
Z-Min	120	3	12
Z-Max	120	3	

Figure 5. Objects in RotCFD.

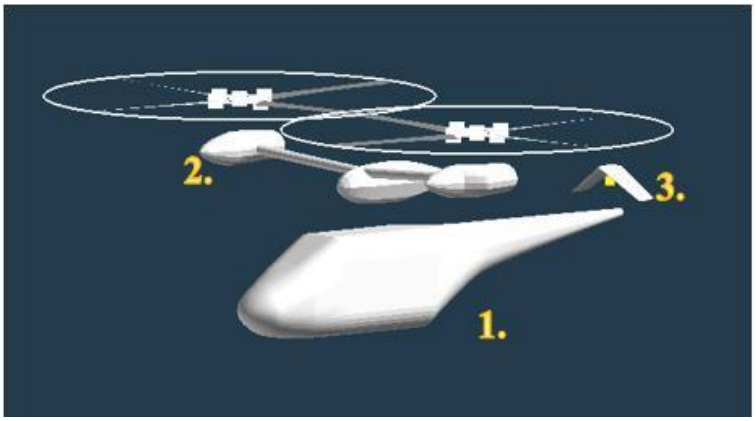

Figure 6. Bodies in RotCFD—exploded view.

2. Grid Study

Before running any official cases for analysis, determining the best grid for the case was crucial. A finer grid provides more detailed and accurate results, but requires a longer amount of time to run. Finding a good balance between accurate results and fast run time is the key to a successful CFD project. The computers provided can handle up to 2.9 million cells; however, these cases run very slowly. In order to find this desirable balance, the recommended method is to start coarse and elevate to finer grids. The time grid also affects the accuracy of results. The main reason for failure of a simulation is a "Turbulence Iteration Diverged," which shows that not enough calculations were being made to accurately keep up with the flow. The best method to resolve this issue is to double the amount of time steps until the flow converges. Iteration count can also be changed; iterations refer to the number of calculations made per time step. The more calculations made, the smoother the results will look.

While performing this grid study, a variety of issues with the setup were discovered. First, no matter how fine the grid and time grid were, the simulations would fail, usually due to "Energy Iteration Failed." This was recognized as a problem with the newer version of RotCFD, known as 402 (Fig. 7). The compressible solver in 402 would activate even when compressibility would not normally be found. Once compressibility activated within the program, the mass residuals would diverge and cause the simulation to fail. Because of this, 401 became the version used for this project. Once results began converging in 401, the true grid study could begin.

Since rotor performance would converge in 402, it was determined that the rotor model was fine at any level of gridding. Forces would also converge at any level of gridding in 401. Many simulations were run at high cell counts, around 2.6 million cells; however, similar results could be attained much faster at a cell count of 1.6 million, so this became the setup for all simulations. Refinement was emphasized around the rotors first, then the bodies (Fig. 8).

The gridding did slightly evolve as simulations went on, with a slightly lower cell count at hover, somewhat higher at 0-, 4-, 8-, and 12-degree angle of attack (AOA), and higher still in specialty cases (Figs. 9, 10). Results seemed consistent across all cases, and only varied by about 300,000 cells on outer regions. Therefore, although this difference exists, it did not impact the results. However, at any cell count, there were still turbulence issues. Doubling the time steps led to convergence at around 20,000 time steps per second. Table 5 documents the refinement level of each box for the different cases, as well as the cell count.

In all cases, rotor and body refinement was kept at 9. Fit bodies was also activated in all cases. This provided tight gridding in necessary areas, and lesser gridding in areas far away. The refinement boxes used for the IGE case feature the same levels, with each of them cut off at –20 on the z-min.

```
Timestep =    1109
Time     =     1.1090000E+00
          ***Compressibility Enabled***
          8 Turbulence Iterations Completed
Timestep =    1110
Time     =     1.1100000E+00
          ***Compressibility Enabled***
          WARNING: Compressible variable flooring performed for 1 cell(s) at iteration 1
          WARNING: Compressible variable flooring performed for 1 cell(s) at iteration 2
          WARNING: Compressible variable flooring performed for 1 cell(s) at iteration 3
          WARNING: Compressible variable flooring performed for 1 cell(s) at iteration 4
          WARNING: Compressible variable flooring performed for 1 cell(s) at iteration 5
          WARNING: Compressible variable flooring performed for 1 cell(s) at iteration 6
          WARNING: Compressible variable flooring performed for 1 cell(s) at iteration 7
          WARNING: Compressible variable flooring performed for 1 cell(s) at iteration 8
          WARNING: Compressible variable flooring performed for 1 cell(s) at iteration 9
          WARNING: Compressible variable flooring performed for 1 cell(s) at iteration 10
          8 Turbulence Iterations Completed
```

Figure 7. Compressibility error in RotCFD 402.

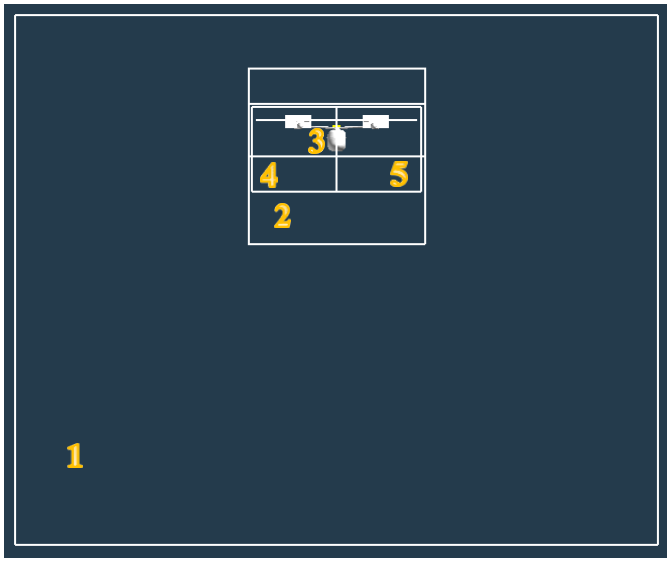

Figure 8. Refinement box locations.

Table 5. Refinement Boxes for Each Case

Case Type	RB1	RB2	RB3	RB4	RB5	Cell #
Hover	3	4	5	6	6	1.313M
FF0, 4, 8, 12	3	4	5	7	7	1.573M
FF6, Other	4	5	6	7	7	1.647M

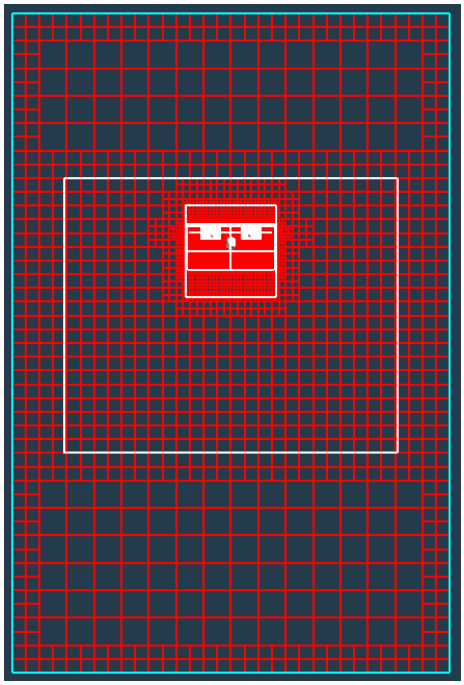

Figure 9. General RotCFD gridding—front view.

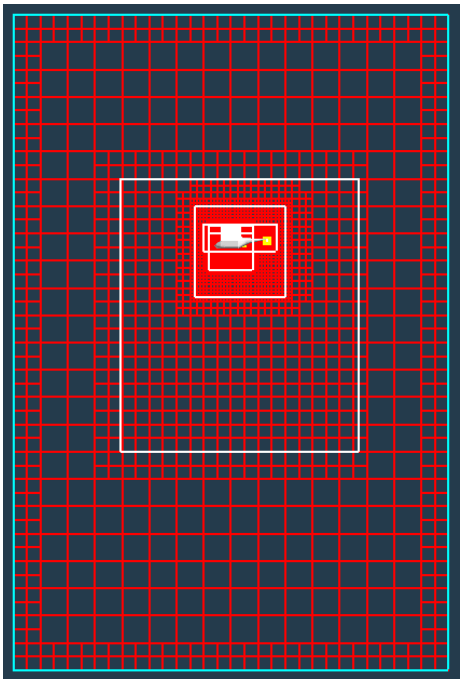

Figure 10. General RotCFD gridding—side view.

3. Case Setup

The hover case for the NR-2 provides a basic frame of reference for the capabilities of the model. In general, the rotors must just produce enough thrust to overcome the DGW of the aircraft. The goal of this simulation was to have rotor wake completely around the body of the aircraft, in order to find the forces created by the rotors acting on the body. The "hover" setting in RotCFD was used for this, with pressure conditions along the walls and a mass outflow correction at the z-min.

A variety of angles were run in order to determine the best operating angle for this model. The angles of 0, 4, 8, and 12 degrees were chosen to be tested for all concept vehicles (see Table 6). However, 6 degrees were added for this model as an additional case. In order to simulate different angles, the general velocity condition in the program was used, with the velocities entered at the different angles. For each wall input, the velocities were inserted. However, a mass outflow was used on the z-max and x-max, except in 0-degree AOA where only the x-mass flow was used.

A handful of "special cases" were run in addition to the main cases listed above. The first case was a confirmation case of the model at its cruise height and 6-degree AOA. This allowed for confirmation of the values generated at sea level. In addition, one simulation was run for climb (see Table 7).

Table 6. Velocities at Different Angles of Attack

Angle of Attack (°)	X-Velocity (ft/s)	Y-Velocity (ft/s)	Z-Velocity (ft/s)
0	194.0	0	0
4	193.5	0	13.50
6	192.9	0	20.23
8	192.1	0	27.00
12	189.8	0	40.33

Table 7. Cases for Analysis

Case	Notation	Description	Total Velocity (ft/s)
1	Hover	Hovering at sea level	0
2	FF0	0° AOA	194
3	FF4	4° AOA	194
4	FF8	8° AOA	194
5	FF12	12° AOA	194
6	FF6	6° AOA	194
7	FF6.1	6° AOA at 5,000 feet	194
8	Climb	Climb OGE	25

RESULTS

The outputs generated from RotCFD that were used for this project are shown below. Only two cases, hover (Figs. 11–15) and forward flight at 8-degree AOA (referred to as FF8) (Figs. 16–20), are shown in the body of this paper. All other cases, including those not analyzed, can be found in Appendix B. Many of the outputs look very similar, with flow visualization looking mostly identical, and the charts having no real meaning other than the convergence values.

Hover Sample Results

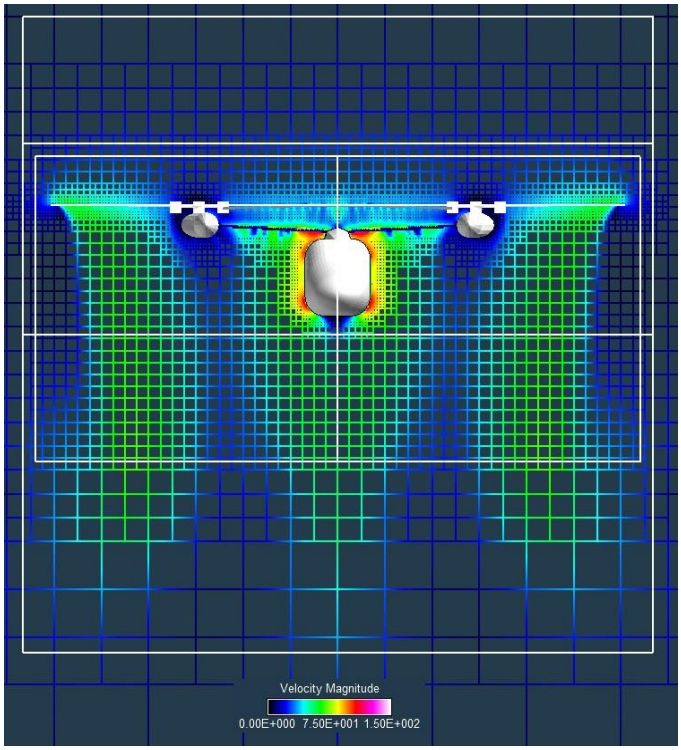

Figure 11. Hover flow visualization.

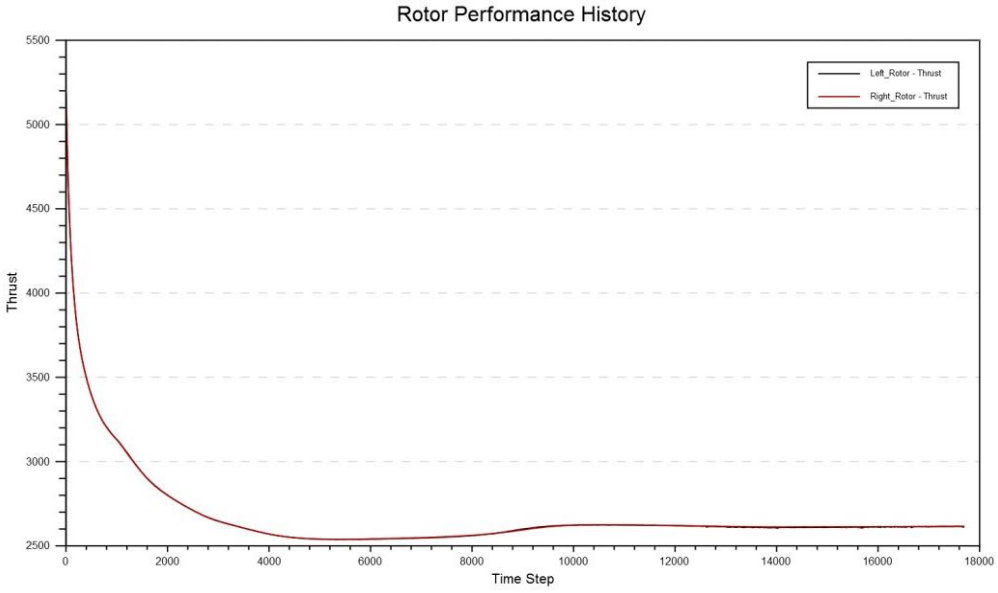

Figure 12. Thrust chart for hover.

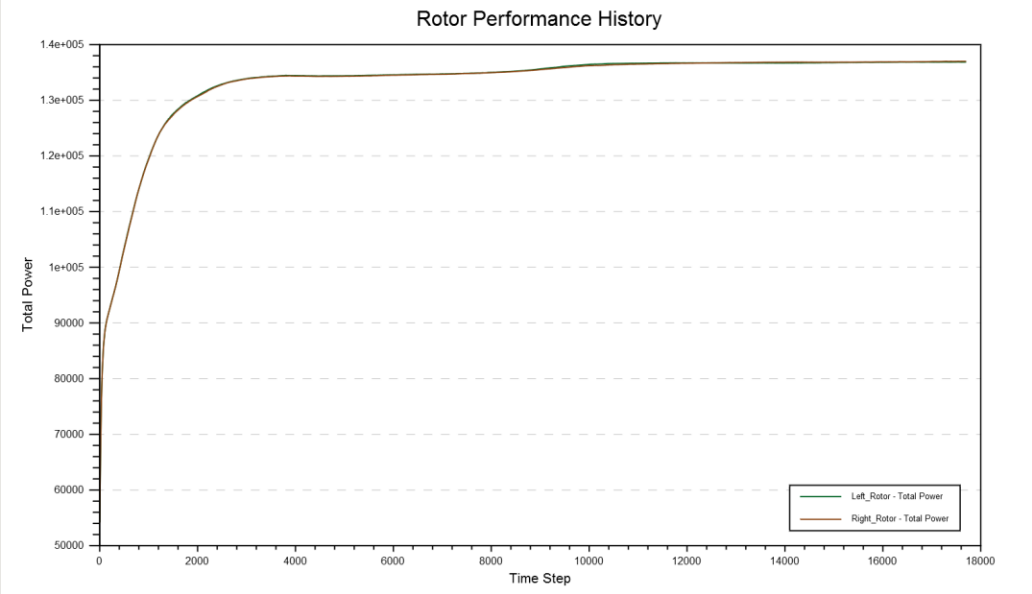

Figure 13. Power chart for hover.

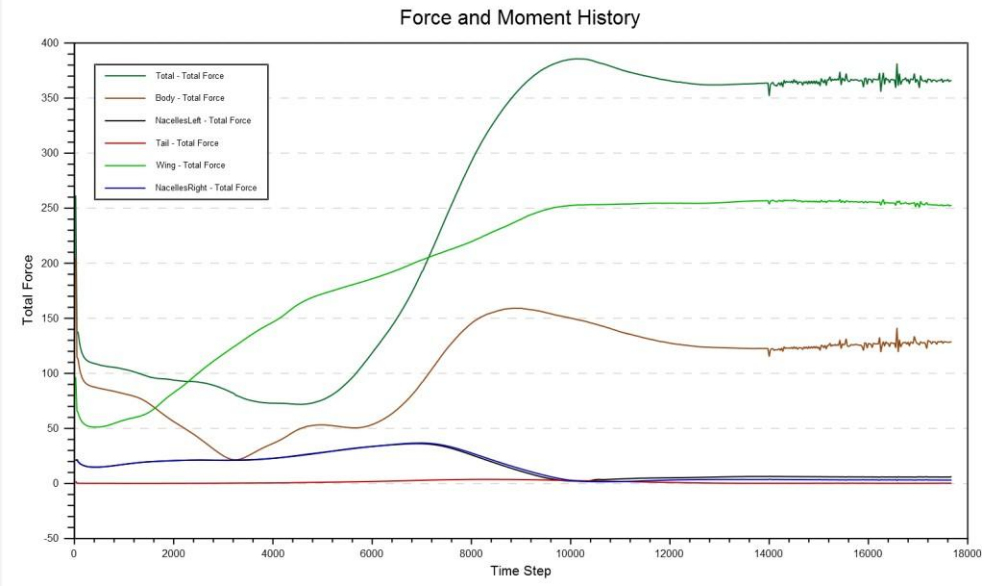

Figure 14. Force and moment chart for hover.

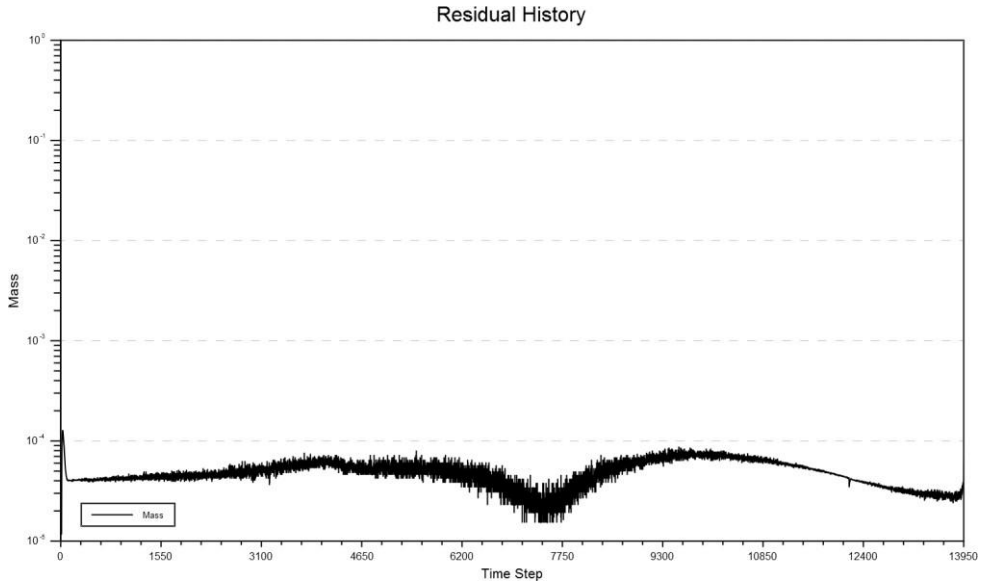

Figure 15. Residuals for hover.

Figure of Merit calculation:

$$Figure\ of\ Merit = \frac{C_T^{3/2}}{\sqrt{2} * C_Q}$$

$From\ RotCFD$: C_T = 0.00827, C_Q = 0.000786

$$Figure\ of\ Merit = \frac{(0.00827)^{3/2}}{\sqrt{2} * (0.000786)} = 0.677$$

Forward Flight Sample Results

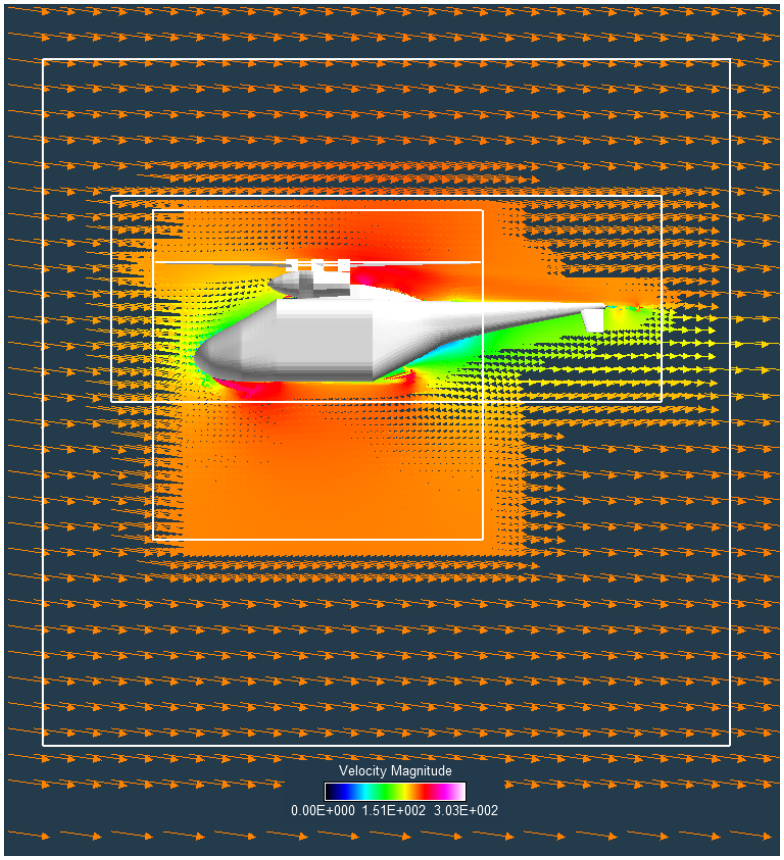

Figure 16. FF8 flow visualization.

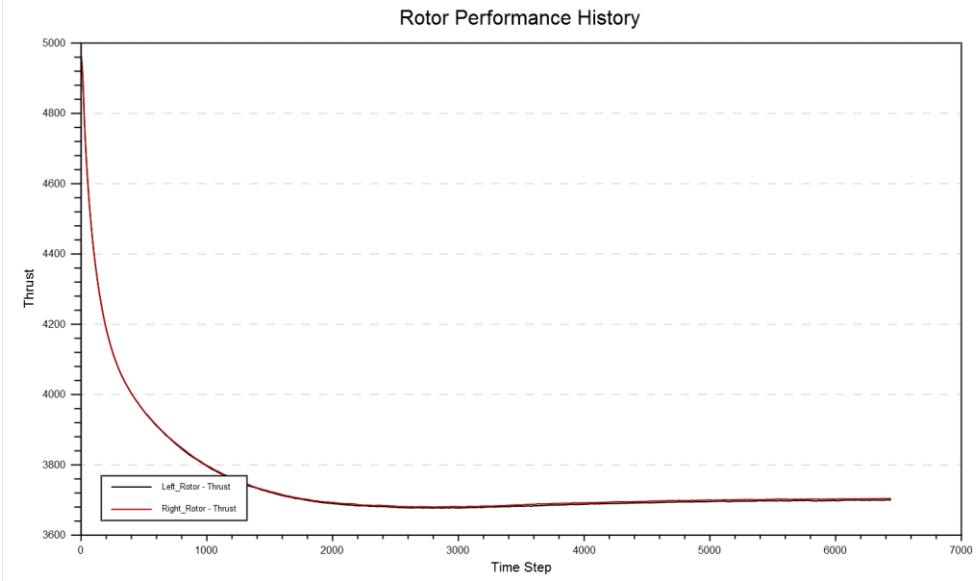

Figure 17. Thrust chart for FF8.

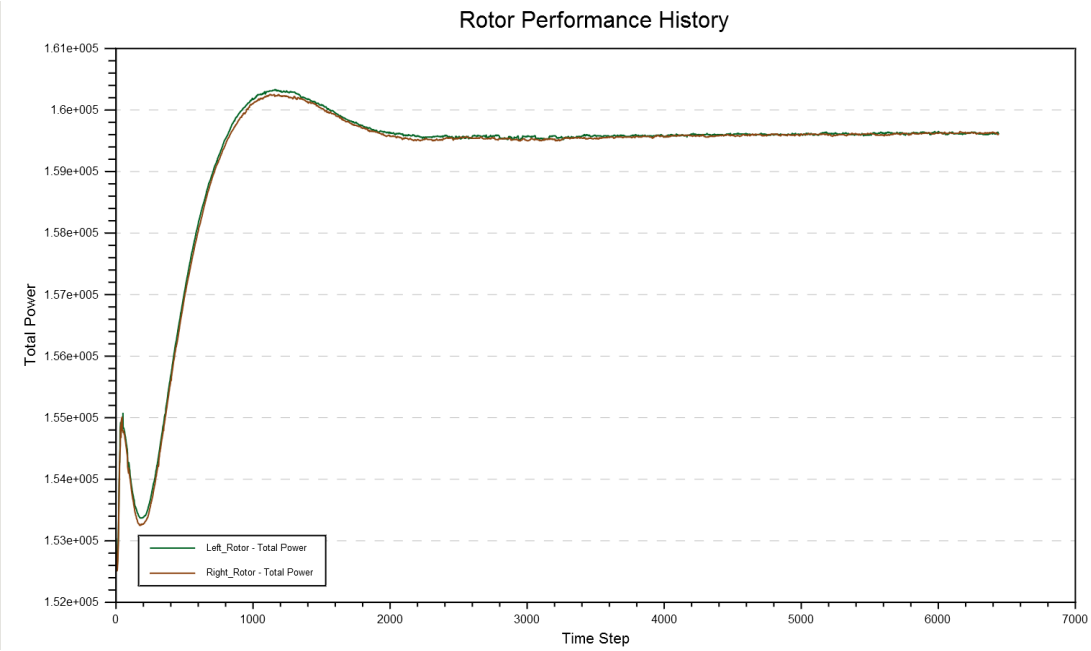

Figure 18. Power chart for FF8.

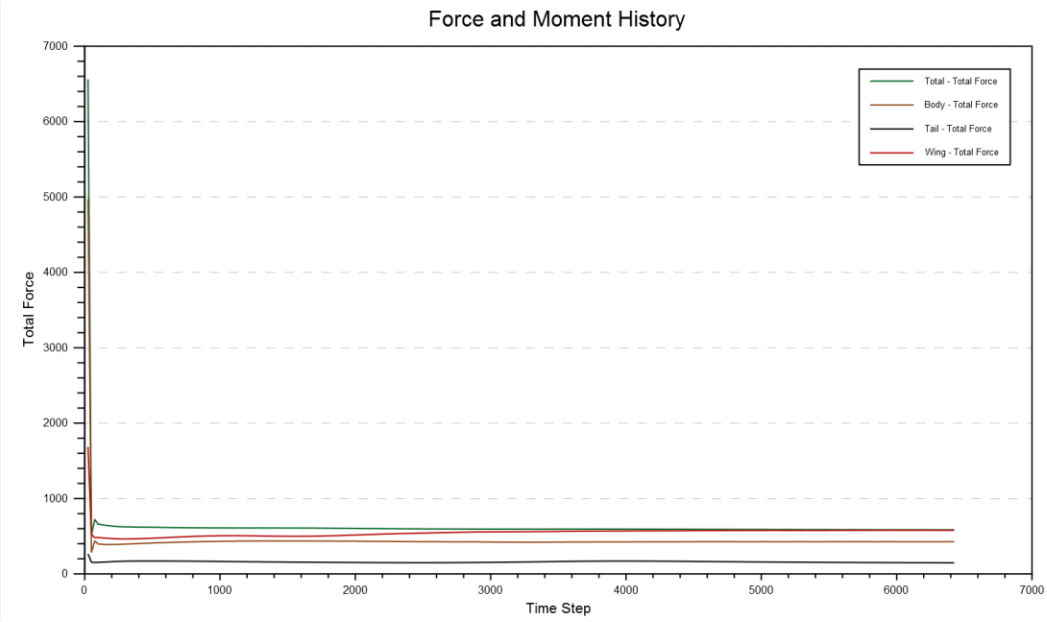

Figure 19. Forces and moments chart for FF8.

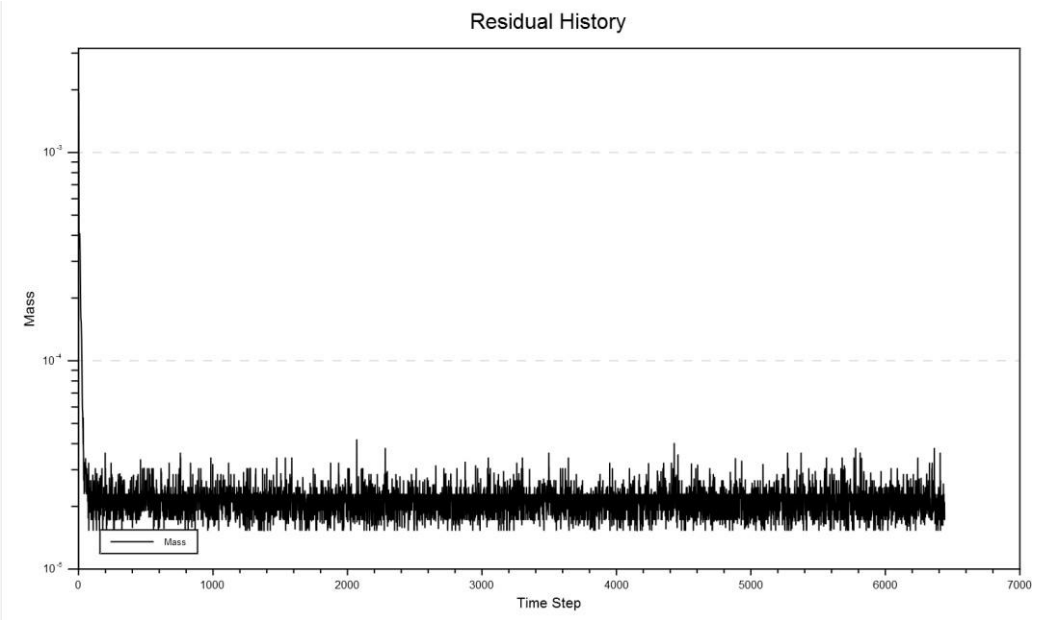

Figure 20. Residuals for FF8.

The numerical outputs for all cases are listed in Table 8. Values were recorded at convergence from each case and placed into the chart. Many of the cases featured drag in both the x- and z-directions. Negative forces in the z-direction indicate drag, while positive values indicate lift. Moments were also briefly noted.

Table 8. Numerical Results from RotCFD

	Hover	FF0	FF4	FF6	FF8	FF12	FF6 5000	Climb
Case#	15	25	18	23	19	20	24	26
Thrust	2600	4726	4219	3956	3691.8	3095	3420	1965.7
Power	135940	128087	148834	155768	159598	158670	135963	113392
Torque	2920	2752	3200	3348	3429	3410	2921	2436
Xforce	35	567.4	571.8	574.9	574.6	518	496.5	-35.3
BodyX	30	170.2	167.866	166.2	162.8	156.4	143.5	22.8
TailX	0	26.9	0	24.3	21.81	17.5	20.3	0
WingX	60	364.8	373.3	384.4	390	344.4	332.7	-57
Zforce	-363	817.6	344.9	71.9	-129	-774.8	100	-354.5
BodyZ	-120	-297.3	-366	-368.9	-391	-441.6	-315.6	-124.3
TailZ	0	0	25.7	-114.8	-157	-232.8	-100	-4.7
WingZ	-254	1121	793	555.7	418.7	-100.4	517.3	-225.6
Roll	0	0	-60	-60	-43	720.6	-57	18.2
Pitch	2250	2141	-101	-1604	-2516	-6372	-971.8	1995.7
Yaw	50	-100	-55	-57	4.68	-136	-22.11	-4

DISCUSSION

The cases can be divided into two main categories based on their wall conditions: hover and velocity. The hover case features only flow generated by the rotors. These cases take a long time to converge because the rotor flow must completely engulf the NR-2 fuselage. This is especially noted in Figure 14, where the forces are changing constantly. This also leads to the residuals being much less predictable.

Velocity cases are much faster and more stable. Because the velocity is completely through the full field at the beginning of the case, everything converges much faster and remains stable. Forces for velocity cases converge almost immediately, and thrust approaches the value soon after. Residuals are stable but contain a decent amount of variation. All the velocity cases were run with 12 iterations, since 10 iterations led to even greater variation in residuals.

The special cases cover a wide range of characteristics. Forward flight at 6-degree AOA, 5,000 feet above sea level behaves exactly like a velocity case. The climb and landing cases, however, contain characteristics of both hover and velocity. Since the velocity is occurring downward through the rotors and is much slower than forward flight, the downwash must once again surround the fuselage in order to get accurate forces. The residuals and thrust/power converge in a similar manner as the velocity cases.

An important note must be made about the 12-degree AOA case. This case was run three times and experienced “Turbulence Iteration Diverged” failure every time. The cases were run with finer gridding and higher time steps, things that normally fix this issue, but the simulation still failed. This points to the notion that the blades were stalling at the high AOA. This is backed up by the fact that zero lift was generated on the wings by this case. The case was still considered because of the fact that all values converged before the turbulence failure, but it is highly unlikely that it would be a realistic configuration for flying. A similar note applies to the 0-degree AOA case. This configuration is not possible for this aircraft, as it cannot fly forward without some AOA greater that zero. By breaking down the forces (as shown in Table 9), is can be seen that there is no forward force to propel the helicopter. Therefore, this is also not a realistic case, but still included based off of convergence.

ANALYSIS

In order to better understand how the NR-2 was behaving, the different forces, lift, thrust, drag and weight, were broken down. In hover and climb/takeoff, this was fairly easy, as all the forces act along the vertical axis. However, in forward flight, the thrust and drag act along the AOA. The same abbreviations described above are used in Table 9.

The first point of analysis is to examine performance characteristics across the areas of attack examined in this study. Figures 21, 22, and 23 show the variation across the five points studied. However, Table 9 can be misleading; it seems that the best arrangement is 0-degree AOA, which has the highest thrust and lowest power, despite not being a realistic case. Therefore, 4-degree AOA has the ideal combination of low power to high thrust. Lift was also generated along the wing (Fig. 24) because of a general airfoil shape. This was also charted across the various AOAs.

Table 9. Forces in Each Direction for NR-2

	Hover	FF0	FF4	FF6	FF8	FF12	FF6 5000	Climb
Angle	0.0	0.0	4.0	6.0	8.0	12.0	6.0	0.0
Radians	0.0	0.0	0.1	0.1	0.1	0.2	0.1	0.0
ThrustUp	5200.0	9452.0	8417.4	7868.7	7311.7	6054.7	6802.5	3931.4
Lift	0.0	1121.0	818.7	555.7	418.7	0.0	517.3	0.0
TotUp	5200.0	10573.0	9236.1	8424.4	7730.4	6054.7	7319.8	3931.4
ThrustFo	0.0	0.0	294.3	413.5	513.8	643.5	357.5	0.0
TotThrust	5200.0	9452.0	8438.0	7912.0	7383.6	6190.0	6840.0	3931.4
UpResult	5200.0	10573.0	9240.8	8434.5	7747.5	6088.8	7328.6	3931.4
Weight	3950.0	3950.0	3950.0	3950.0	3950.0	3950.0	3950.0	3950.0
DragDn	-363.0	297.3	366.0	483.7	548.0	774.8	415.6	354.6
TotDown	3587.0	4247.3	4316.0	4433.7	4498.0	4724.8	4365.6	4304.6
DragBk	35.0	567.4	571.8	574.9	574.6	518.0	496.5	-35.3
TotDrag	364.7	640.6	678.9	751.3	794.0	932.0	647.5	356.4
DnResult	3587.2	4285.0	4353.7	4470.8	4534.6	4753.1	4393.7	4304.7

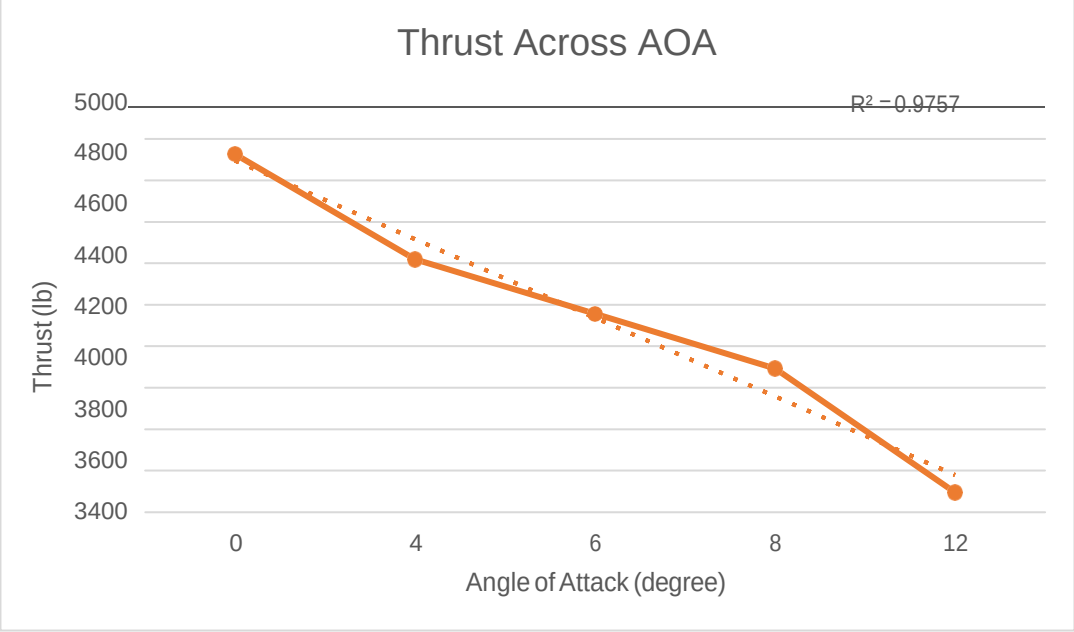

Figure 21. Thrust values at different angles of attack.

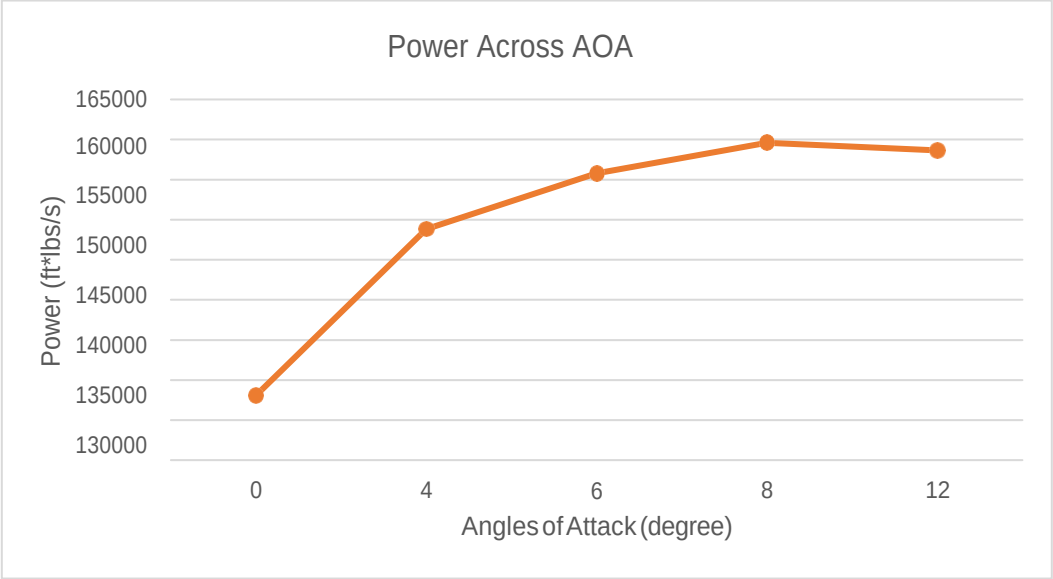

Figure 22. Power values at different angles of attack.

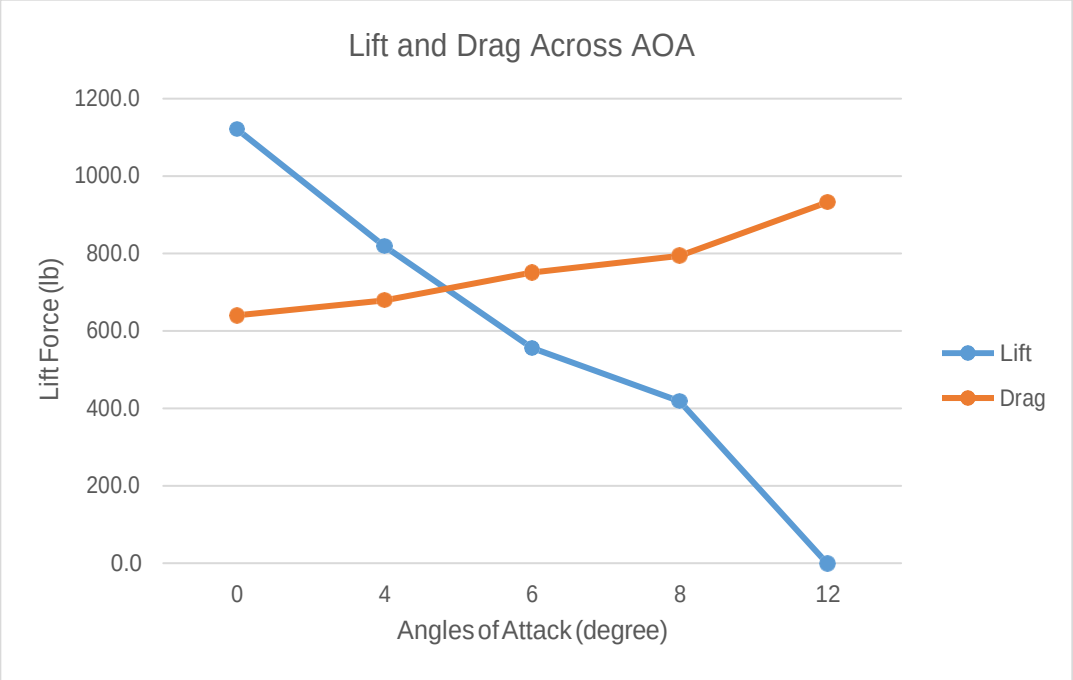

Figure 23. Lift and drag at different angles of attack.

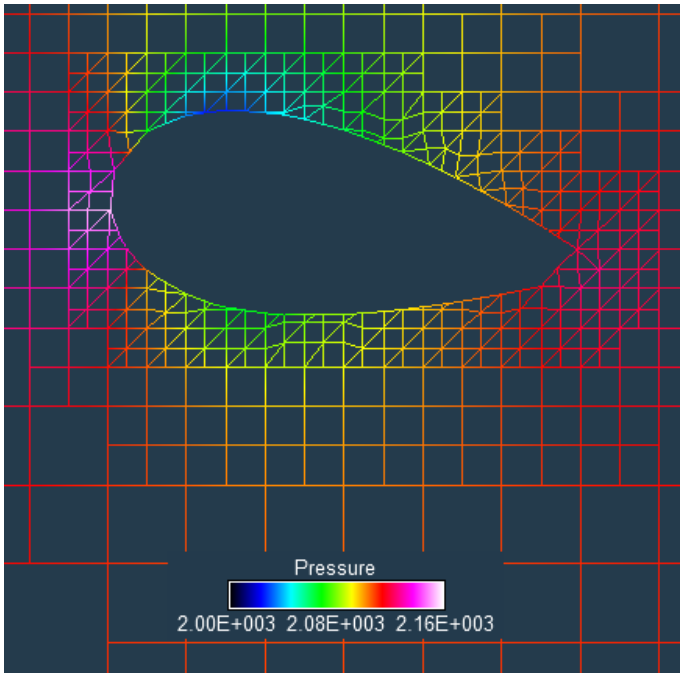

Figure 24. Pressure around wing at FF4.

Pitching moment is another important aspect to forward flight (Fig. 25). Although there are other moments occurring on the body, the values are small and mostly negligible. A negative pitching moment indicates the tendency for the nose of the aircraft to turn upward, while a positive moment turns the nose downward. For a helicopter in forward flight, it is better for the nose to tend upward. Since the nose is pushed down in forward flight, stability should tend the nose up. Therefore, AOAs with negative pitching moments are ideal, which eliminates 0-degree AOA.

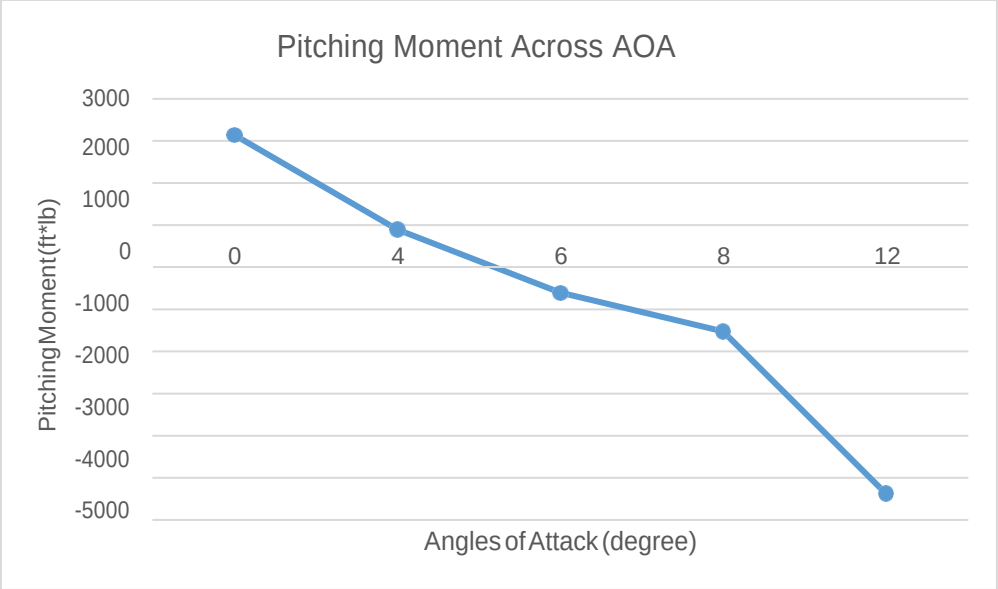

Figure 25. Pitching moment at different angles of attack.

The next step was to separate the important forces from the more negligible ones. All configuration cases were considered at this time; however, since there was already a 6-degree AOA case, the case at 5,000 feet was ignored for analysis. This case and the other 6-degree AOA case will be compared directly. Since weight is a constant downward force, no matter the AOA, it does not need to be listed in every section. In addition, even though the connection between the two rotors on the model is wing-shaped and does generate lift in some cases, it is not as significant as the other values. Thrust and drag both occur along the AOA, and vary significantly between cases (see Table 10).

Table 10. Thrust and Drag Values for All Cases

Case	Thrust (lb)	Drag (lb)
Hover	5,200	364.7
FF0	10,573	640.6
FF4	9,236	678.9
FF6	8,424	751.3
FF8	7,730	794.0
FF12	6,054	932.0
Climb	3,931	356.4

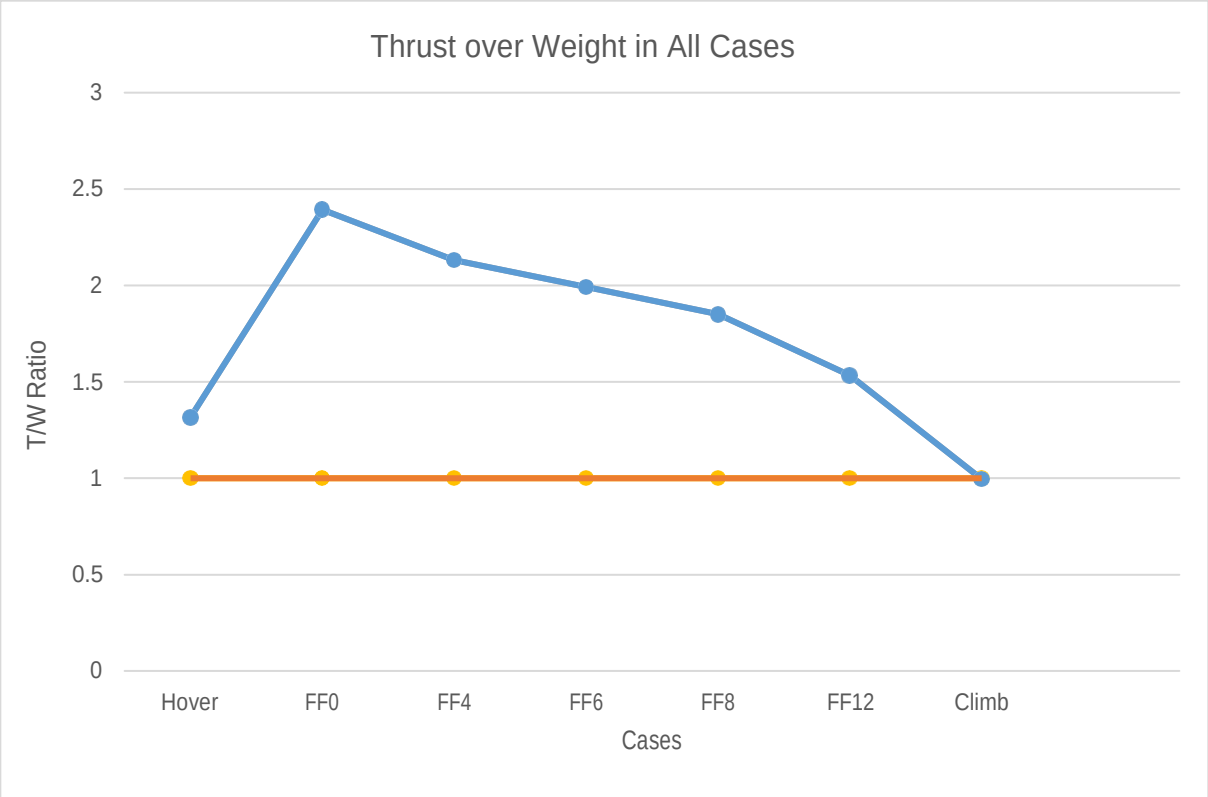

Figure 26. Thrust-over-weight graph.

Comparing upward thrust to weight is one the most basic indicators of helicopter performance (Fig. 26). There must be more upward thrust (T) from the rotors than there is downward weight (W), or the helicopter is unable to support itself in the air. A minimum goal of 1 for T/W ratio was set, as this means the helicopter is producing exactly enough thrust to support itself. One case, climb, fell below this requirement. However, this would likely be corrected by raising the collective pitch, which is how a regular helicopter would execute this type of maneuver.

One last comparison point for all cases is the summation of the different forces (Fig. 27). Positive forces are those that keep the helicopter in its desired maneuver, such as forward flight. Negative forces are those that resist the desired motion. In a non-accelerating case, these forces should be balanced, with the helicopter moving in the desired direction. More positive force than negative indicates acceleration, while more negative force than positive means that the helicopter is failing the maneuver. Climb, once again, is the only case that falls below this threshold.

The final comparison to be made is comparing both forward flight cases at 6-degree AOA (Fig. 28). The difference between each value was 15 percent. However, since all the values involved went down, the general performance of NR-2 is still valid at sea level. Therefore, the performance characteristics determined in this project are reasonable.

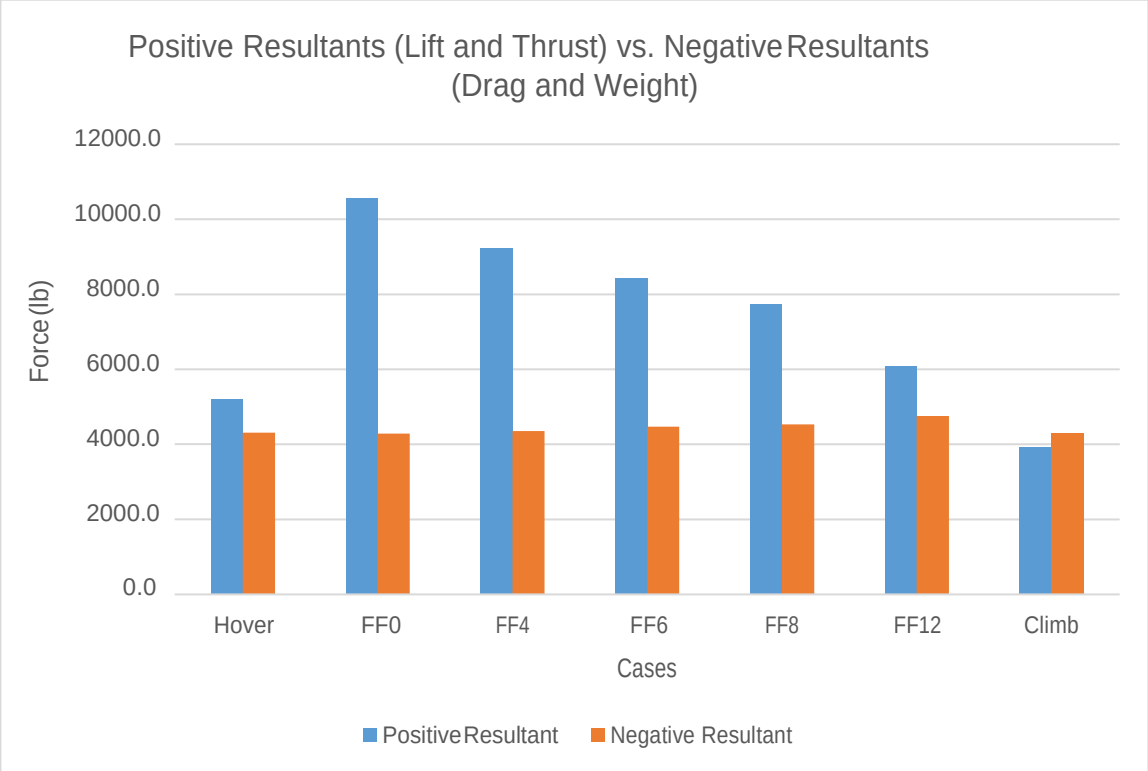

Figure 27. Resultant forces across all cases.

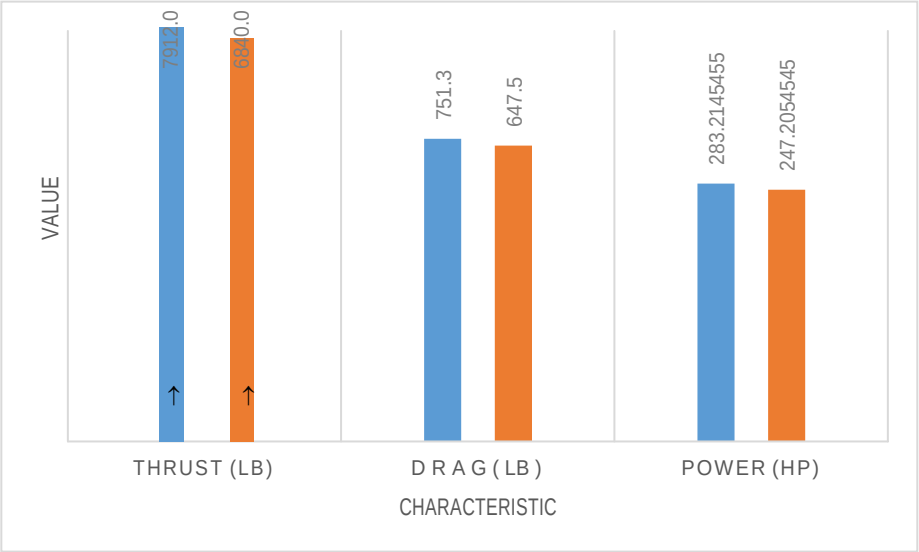

Figure 28. Differences in output at 0 and 5,000 feet at 6-degree AOA.

CONCLUSIONS

The NASA Reference Model 2 (NR-2) shows great potential as a future VTOL for urban air mobility (UAM). The rotors are capable of producing significant thrust, enough to overcome the 3,950-pound DGW for the aircraft, as well as the drag generated in flight. This is improved on by the small amount of lift generated by the wings between the two rotors. Studying the various AOAs shows that the ideal configuration for flight of this aircraft falls around 4-degree AOA, and any increase also increases the power while decreasing the thrust. All configurations except one met the minimum performance requirements in order to complete the maneuver.

Knowledge of basic helicopter controls improves understanding of results. As this is a fully articulated helicopter, the collective pitch can be adjusted to meet the thrust and power requirements of the maneuver being performed. Since a general operating collective pitch was used for all maneuvers, at a value that falls below the general limits of a helicopter, results were not fully accurate for all cases. However, the ability to more easily change the collective and cyclic pitch of the rotors would provide more accurate results. Fine tuning the pitch to get performance characteristics closer to actual ratios of values would improve the results of this project. This would likely change the true AOA ideal for the NR-2, as enough thrust would be generated at a lower collective pitch.

FUTURE WORK

A variety of work can still be performed on the NR-2. Several more maneuvers can be simulated using RotCFD to get a more thorough understanding of the model. For example, no turning maneuvers were simulated, which would provide different performance characteristics than pure forward flight. Simulating could also be done using unsteady rotors, which is a time-consuming but more realistic simulation. Performing a pitch sweep on the rotor to find the best angle for certain maneuvers would also be useful. Other simulations could also be rerun, with higher gridding or longer time steps. This could potentially yield more accurate results.

Now that general performance characteristics have been proven, the model can also be refined to work better. Once the model has been refined, then other testing can be done. Small-scale wind tunnel testing can be performed on a model, or rotor testing can begin. Small-scale wind tunnel testing is another way to prove the performance of the model. Previous work has shown a reasonable level of accuracy between testing and simulating. Beyond that, further full-scale development and testing can progress.

BIBLIOGRAPHY

R. G. Rajagopalan, V. Baskaran, A. Hollingsworth, A. Lestari, D. Garrick, E. Solis, and B. Hagerty, "RotCFD - A tool for Aerodynamic Interference of Rotors: Validation and Capabilities." AHS International - Future Vertical Lift Aircraft Design Conference, Jan. 18–20, 2012, San Francisco, CA, pp. 311-327.

W. Johnson, C. Silva, and E. Solis, "Concept Vehicles for VTOL Air Taxi Operations." AHS Technical Conference on Aeromechanics Design for Transformative Vertical Flight, San Francisco, CA, Jan. 16–19, 2018.

W. J. F. Koning, C. Russell, E. Solis, and C. Theodore, "Mid-Fidelity Computational Fluid Dynamics Analysis of the Elytron 4S UAV Concept," NASA/TM-2018-219788, Nov. 2018.

APPENDIX A: RAW DATA

Table A1. Abbreviations in Raw Data Charts

Abbreviation	Meaning
Turb	turbulence diverge
Velocity	cruise speed (194)
R	residuals
F	no results bc fail
CW	clockwise
energy	energy diverge
spike	crazy residuals
	bad
	okay
	good
conv	converged

Table A2. Raw Data Charts

	Case1	Case2	Case3	Case4	Case5	Case6	Case7	Case8	Case9	Case10
BODIES										
# Bodies	4	4	4	4	4	4	4	4	4	4
Refinement	9	9	9	9	9	9	9	9	9	9
Forces	4	4	4	4	4	4	4	4	4	4
ROTORS										
Pitch	10	10	10	10	10	10	10	10	10	10
Position	9,11,5.5	9,11,5.5	9,11,5.5	9,11,5.5	9,11,5.5	9,11,5.5	9,11,5.5	0,11,0	0,11,0	0,11,0
Refinement	9	9	9	9	9	9	9	9	9	9
BOUNDARY										
Lower										
X	-25	-25	-25	-50	-50	-50	-50	-120	-120	-120
Y	-50	-50	-50	-100	-100	-100	-100	-120	-120	-120
Z	-50	-50	-50	-100	-100	-100	-100	-240	-240	-240
Upper										
X	75	75	75	150	150	150	150	120	120	120
Y	50	50	50	100	100	100	100	120	120	120
Z	50	50	50	100	100	100	100	120	120	120
Wall Conditions	Pressure	Pressure	Pressure	Pressure	Pressure	Pressure	Pressure	Pressure	Pressure	Velocity
Flight Conditions	Hover	Hover	Hover	Hover	Hover	Hover	Hover	Hover	Hover	FF(slow)
Angle of Attack	0	0	0	0	0	0	0	0	0	0
Edge Refinement	1	1	1	1	1	1	1	1	1	4
Rbox #	4	4	4	4	4	4	5	5	5	5
Rbox Scale	5,6,8	5,6,8	5,6,8	5,6,7	5,6,7	5,6,7	4,5,6,7	4,5,6,7	4,5,6,7	4,5,6,7
SOLVER										
Version	402	402	402	402	402	402	402	401	401	401
Cell Count	2.248M	2.248M	265	1.100M	1.100M	2.239M	1.696M	2.239M	2.686M	2.686M
Time Length	10	10	5	5	5	5	10	5	5	1
Time Steps	10000	15000	500	5000	1000	10000	10000	10000	10000	10000
Iterations	10	10	10	10	10	10	10	10	10	10
Restart Int.	250	250	250	250	250	250	250	250	250	250
Solver Int.	100	100	100	100	100	50	100	25	25	100
OUTPUT										
Completed TS	1400	1445	368	1677	63	1435	1564	2911	2893	3564
Thrust	400	400	400	400	F	400	400	400	400	925
Power	20000	20000	20000	20000	F	20000	20000	20000	20000	19000
Torque	-	-	-	-	-	-	-	420	420	410
Body Force	20	17.5	F	49	F		F	12.6	12.6	259
Residuals Good?	N	N	N	N	N	M	N	Y	Y	Y
Complete?	N	N	N	N	N	N	N	N	Y	Y
Stop Reason	turb	turb	energy	energy	spike	manual	energy	turb	turb	manual
Comment						R @ 1000				

Table A2. Raw Data Charts (continued)

	Case11	Case12	Case13	Case14	Case15	Case16	Case17	Case18	Case19	Case20
BODIES										
# Bodies	5	5	5	5	5	5	5	3	3	3
Refinement	9	9	9	9	9	9	9	9	9	9
Forces	5	5	5	5	5	5	5	3	3	3
ROTORS										
Pitch	10	10	10	20	20	20	20	20	20	20
Position	0,11,0	0,11,0	0,11,0	0,11,0	0,11,0	0,11,0	0,11,0	0,11,0	0,11,0	0,11,0
Refinement	9	9	9	9	9	9	9	9	9	9
BOUNDARY										
Lower										
X	-120	-120	-120	-120	-120	-120	-120	-120	-120	-120
Y	-120	-120	-120	-120	-120	-120	-120	-120	-120	-120
Z	-240	-240	-240	-240	-240	-240	-240	-240	-240	-240
Upper										
X	120	120	120	120	120	120	120	120	120	120
Y	120	120	120	120	120	120	120	120	120	120
Z	120	120	120	120	120	120	120	120	120	120
Wall Conditions	Velocity	Velocity	Pressure	Pressure	Pressure	Velocity	Velocity	Velocity	Velocity	Velocity
Flight Conditions	FF	FF	Hover	Hover	Hover	FF	FF	FF	FF	FF
Angle of Attack	0	4	0	0	0	4	8	4	8	12
Edge Refinement	4	4	4	4	4	3	3	3	3	3
Rbox #	5	5	5	5	5	5	5	5	5	5
Rbox Scale	4,5,6,7	4,5,6,7	4,5,6,7	4,5,6,7	3,4,5,6	3,5,6,7	3,5,6,7	3,5,6,7	3,5,6,7	3,5,6,7
SOLVER										
Version	401	401	401	401	401	401	401	401	401	401
Cell Count	2.686M	2.686M	2.686M	2.686M	1.313M	1.573M	1.573M	1.573M	1.573M	1.573M
Time Length	1	1	2	2	2.5	2	2	2	2	2
Time Steps	15000	15000	30000	30000	20000	40000	40000	40000	40000	40000
Iterations	10	10	10	10				12	12	
Restart Int.	250	250	250	250	250	250	250	250	250	250
Solver Int.	100	100	100	100	100	100	100	100	100	100
OUTPUT										
Completed TS	3876	12375			17699	14000		4000	6441	2132
Thrust	1250	1250		2600	2600			4219	3691.8	
Power	18750	F			135940			148834	159598	
Torque	400	400			2920			3200	3429.9	
Body Force	1045	1040			363			668.5	594.6	932
Residuals Good?	M	Y			Y	y	y	y	Y	
Complete?	Y	Y			Y	y	y	Y	Y	
Stop Reason	manual	memory T			turb	conv	conv	conv	conv	
Comment		unequal			R@14000	bad aoa	bad aoa			

Table A2. Raw Data Charts (concluded)

	Case21	Case22	Case23	Case24	Case25	Case26	Case27
BODIES							
# Bodies	3	3	3	3	3	3	3
Refinement	9	9	9	9	9	9	9
Forces	3	3	3	3	3	3	3
ROTORS							
Pitch	20	20	20	20	20	20	20
Position	0,11,0	0,11,0	0,11,0	0,11,0	0,11,0	0,11,0	0,11,0
Refinement	9	9	9	9	9	9	9
BOUNDARY							
Lower							
X	-120	-120	-120	-120	-120	-120	-120
Y	-120	-120	-120	-120	-120	-120	-120
Z	-240	-240	-240	-240	-240	-240	-240
Upper							
X	120	120	120	120	120	120	120
Y	120	120	120	120	120	120	120
Z	120	120	120	120	120	120	120
Wall Conditions	Velocity	Velocity	Velocity	Velocity	Velocity	Velocity	Velocity
Flight Conditions	FF	FF	FF	FF	FF	Takeoff	Landing
Angle of Attack	12	12	6	6	0	0	0
Edge Refinement	3	3	3	3	3	3	3
Rbox #	5	5	5	5	5	5	5
Rbox Scale	3,5,6,7	4,5,6,7	4,5,6,7	4,5,6,7	4,5,6,7	4,5,6,7	4,5,6,7
SOLVER							
Version	401	401	401	401	401	401	401
Cell Count	1.573M	1.573M	1.647M	1.647M	1.573M	1.647M	1.552M
Time Length	2	1	2	2	2	2	2
Time Steps	40000	20000	40000	40000	40000	40000	40000
Iterations	12	15	12	12	12	12	12
Restart Int.	250	250	250	250	250	250	250
Solver Int.	100	100	100	100	100	100	100
OUTPUT							
Completed TS	1800	2000	-	-	1000	19250	
Thrust							
Power							
Torque							
Body Force							
Residuals Good?				Y			
Complete?				Y			
Stop Reason				conv			
Comment				5000ft			

APPENDIX B: ROTCFD RESULTS

1. Successful Cases

Case 15 (Hover):

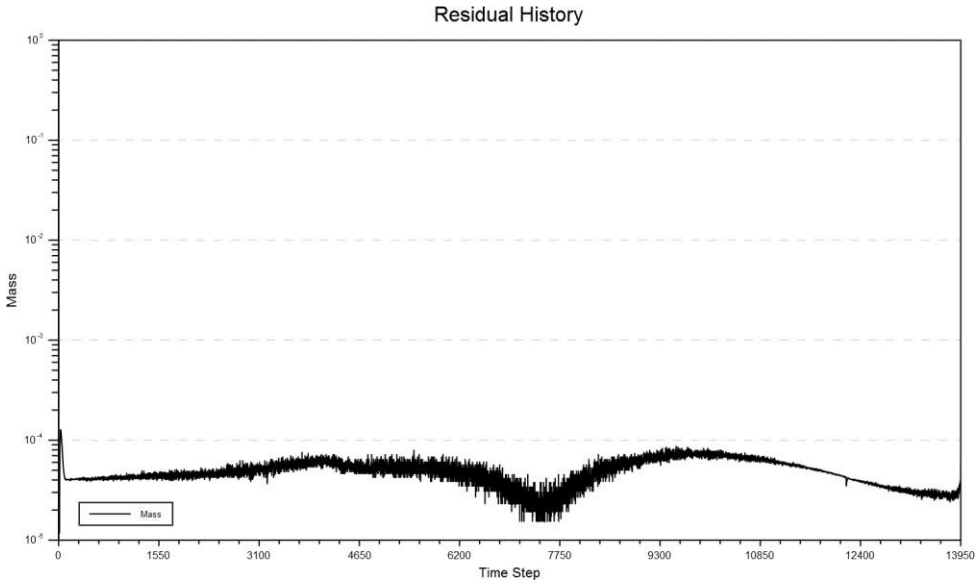

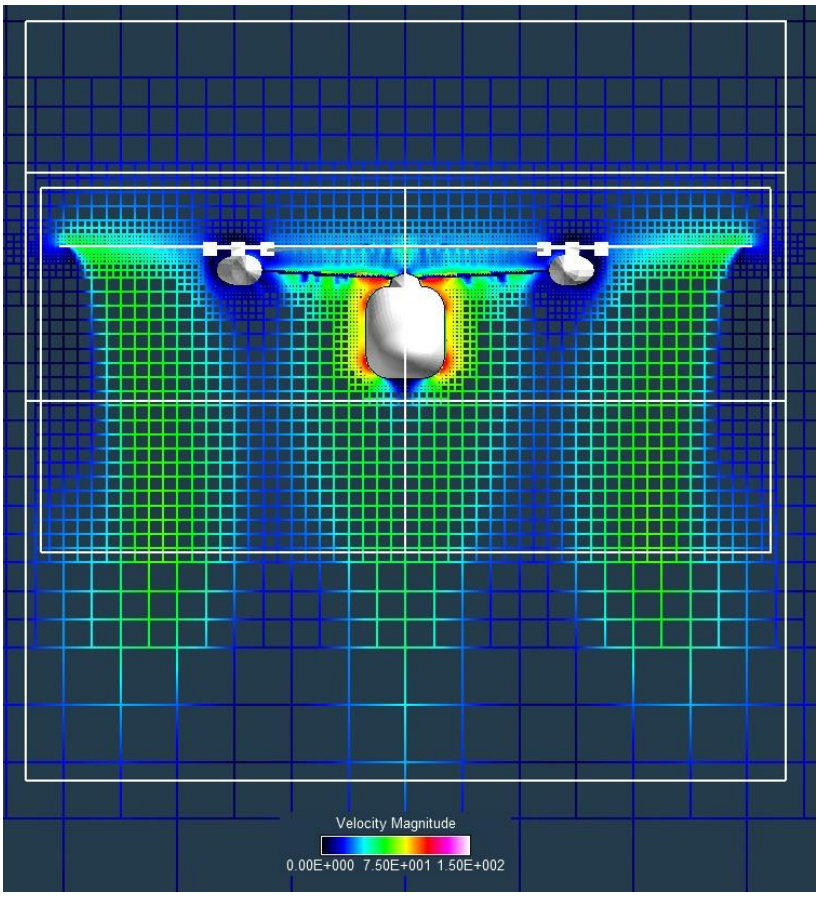

Case 25 (FF0):

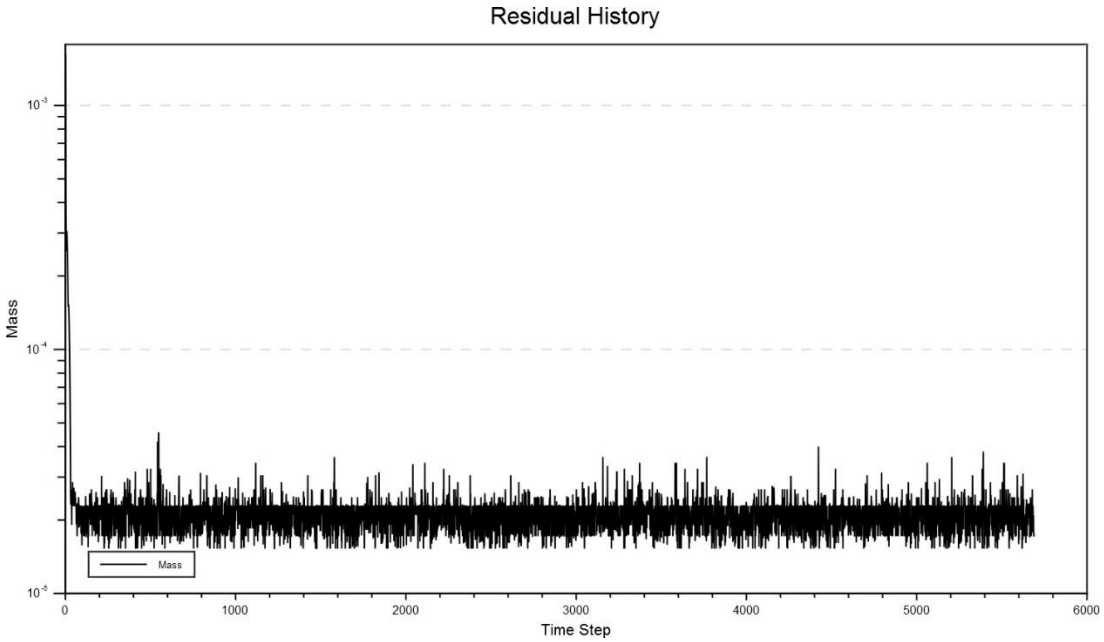
Residual History
Mass
Time Step
Mass
0
1000
2000
3000
4000
5000
6000

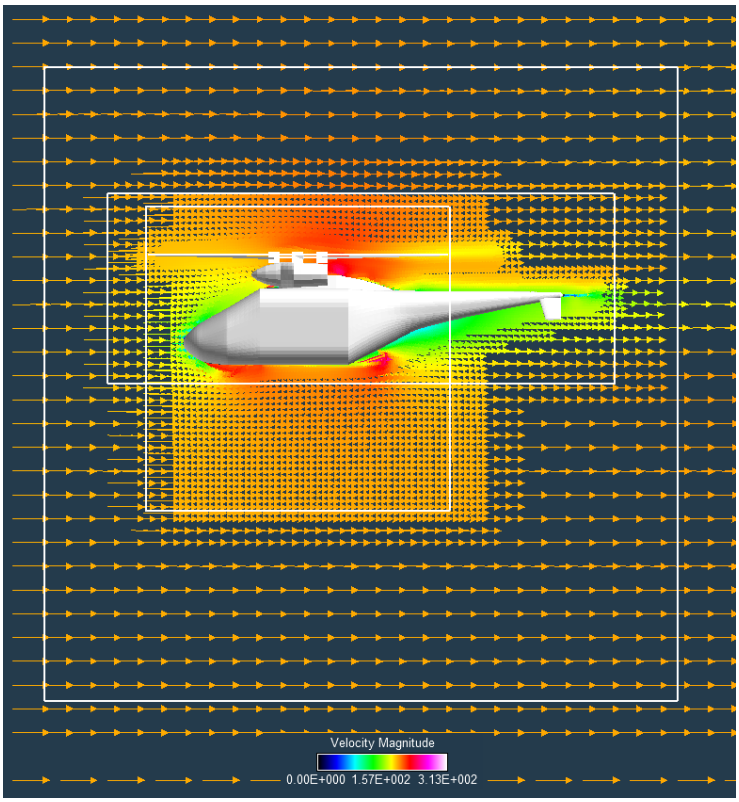
Velocity Magnitude
0.00E+000 1.57E+002 3.13E+002

Case 18 (FF4):

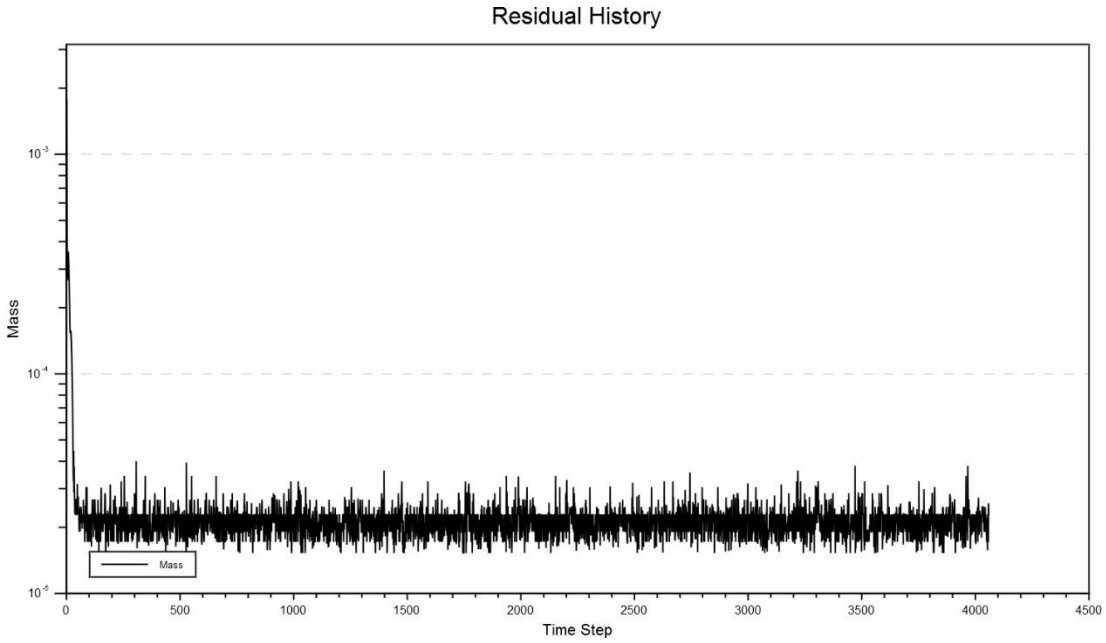
Residual History
Mass
Time Step
Mass
10-3
10-4
10-5
0
500
1000
1500
2000
2500
3000
3500
4000
4500

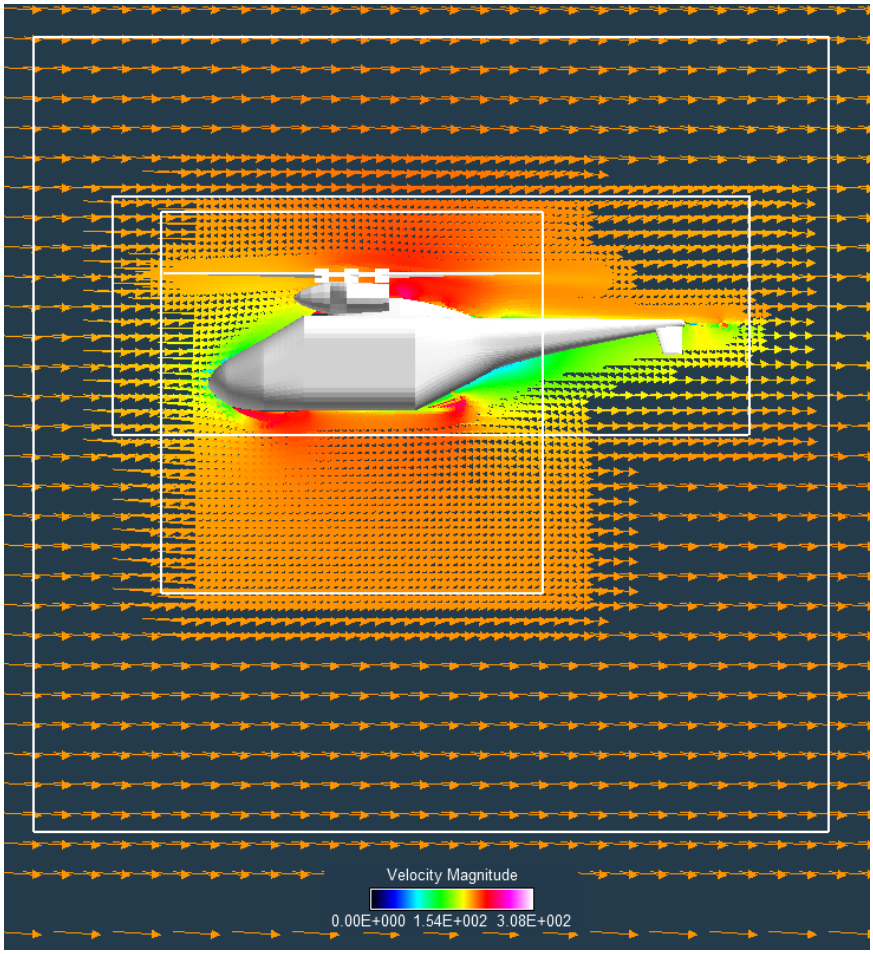
Velocity Magnitude
0.00E+000 1.54E+002 3.08E+002

Case 23 (FF6):

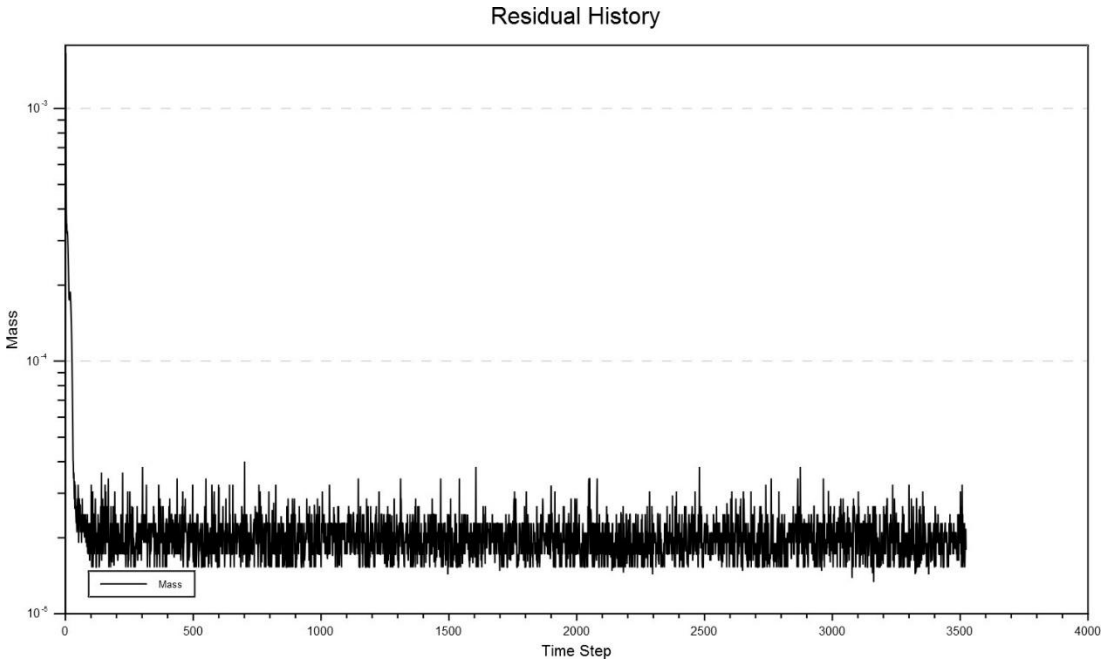
Residual History
Mass
Time Step
Mass
0
500
1000
1500
2000
2500
3000
3500
4000

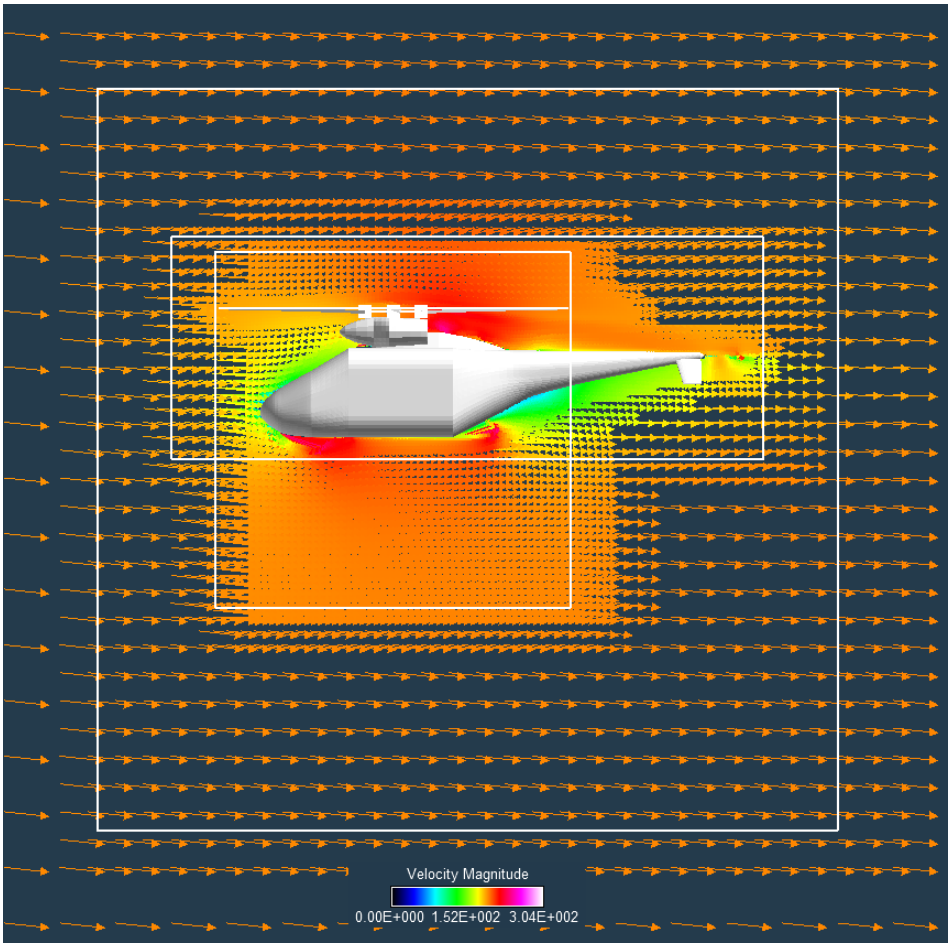
Velocity Magnitude
0.00E+000 1.52E+002 3.04E+002

Case 19 (FF8):

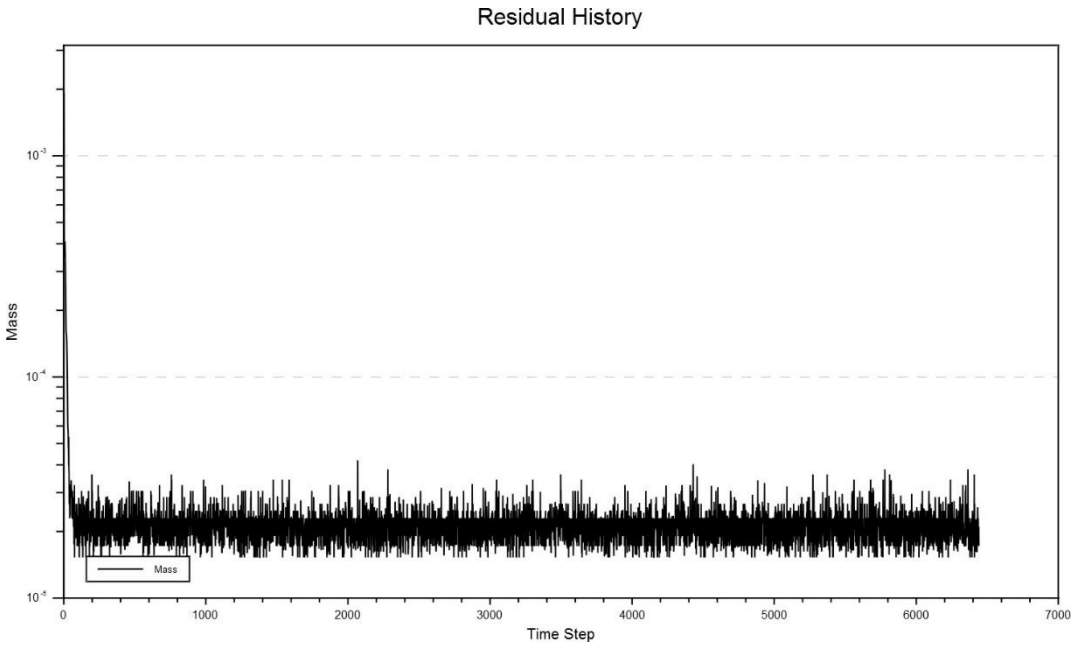
Residual History
Mass
Time Step
Mass
0
1000
2000
3000
4000
5000
6000
7000

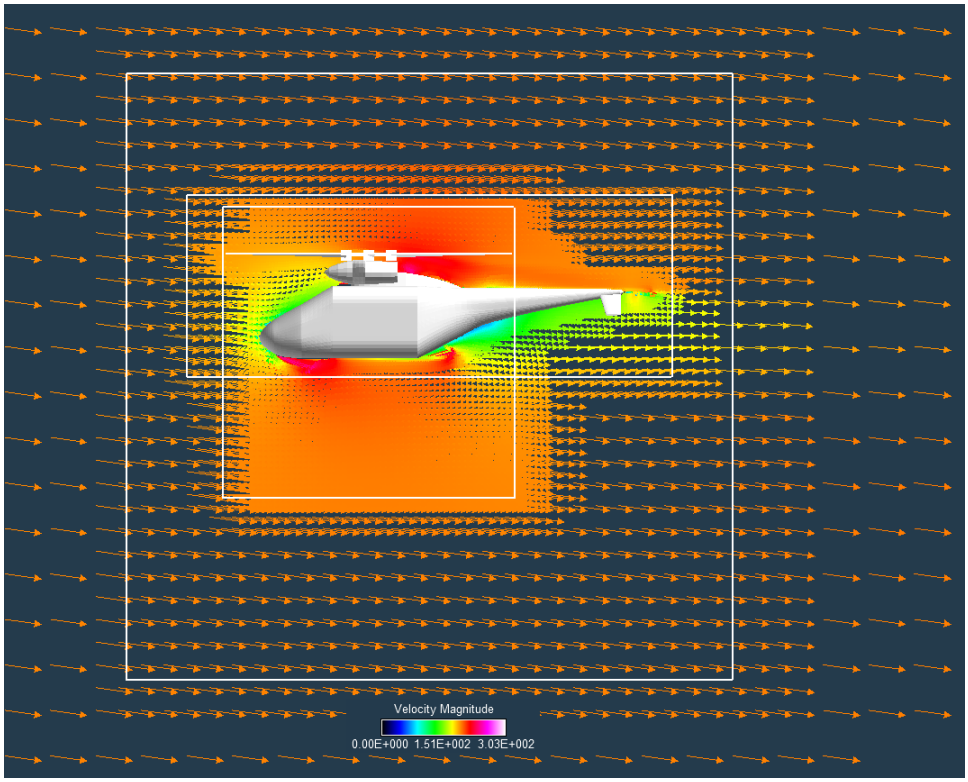
Velocity Magnitude
0.00E+000 1.51E+002 3.03E+002

Case 20 (FF12):

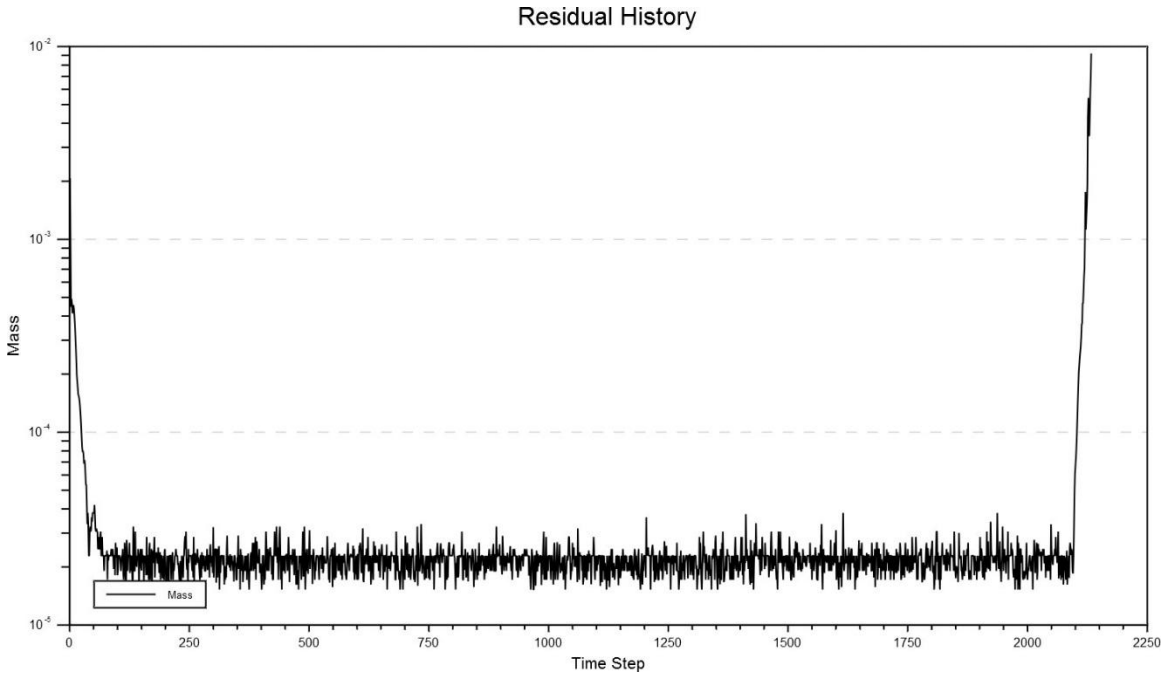
Residual History
Mass
Time Step
Mass
10^-2
10^-3
10^-4
10^-5
0
250
500
750
1000
1250
1500
1750
2000
2250

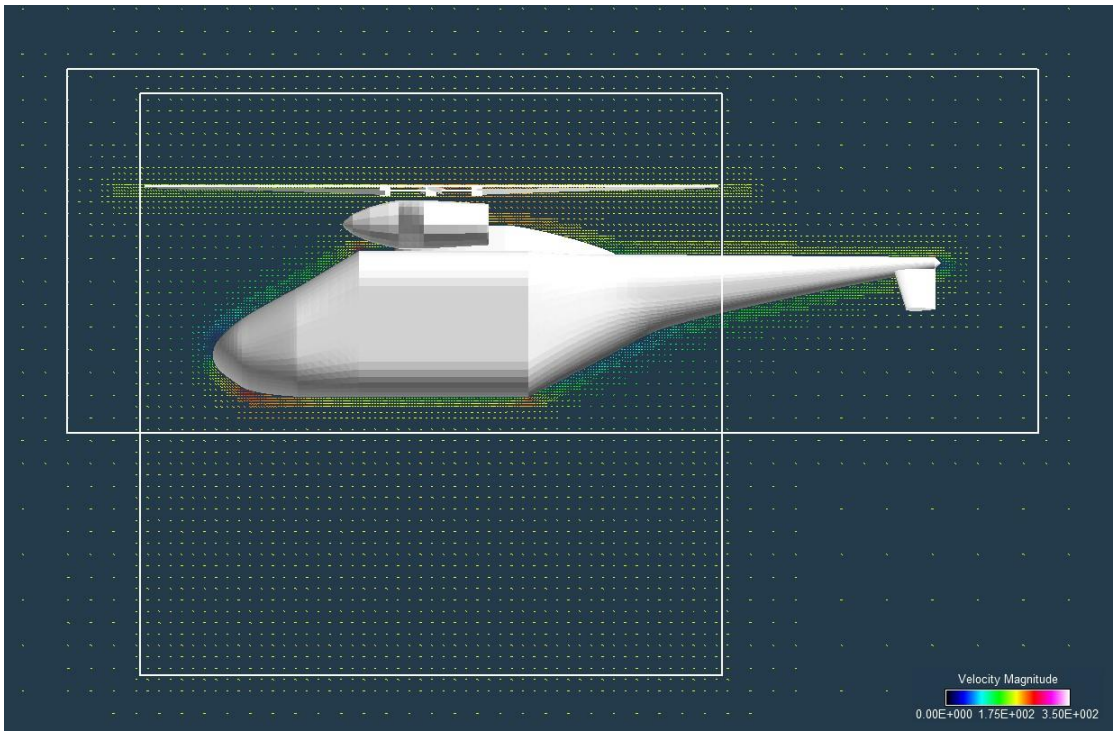
Velocity Magnitude
0.00E+000 1.75E+002 3.50E+002

Case 26 (Climb):

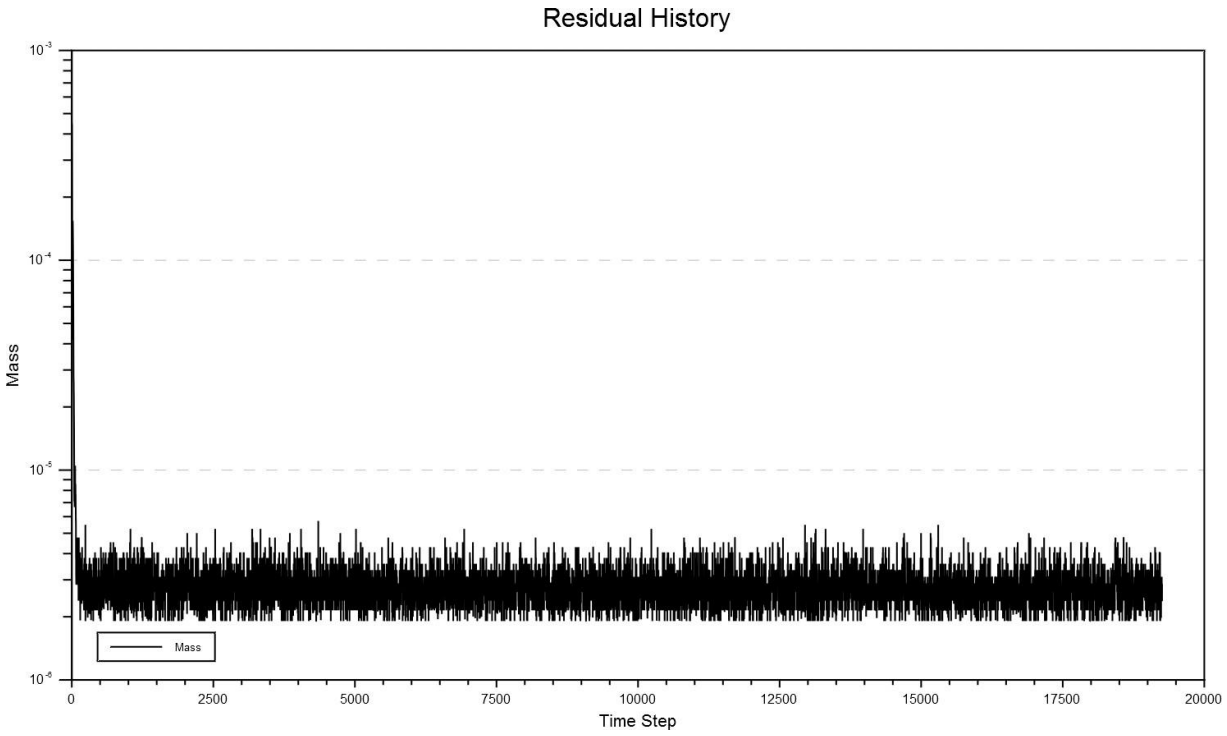

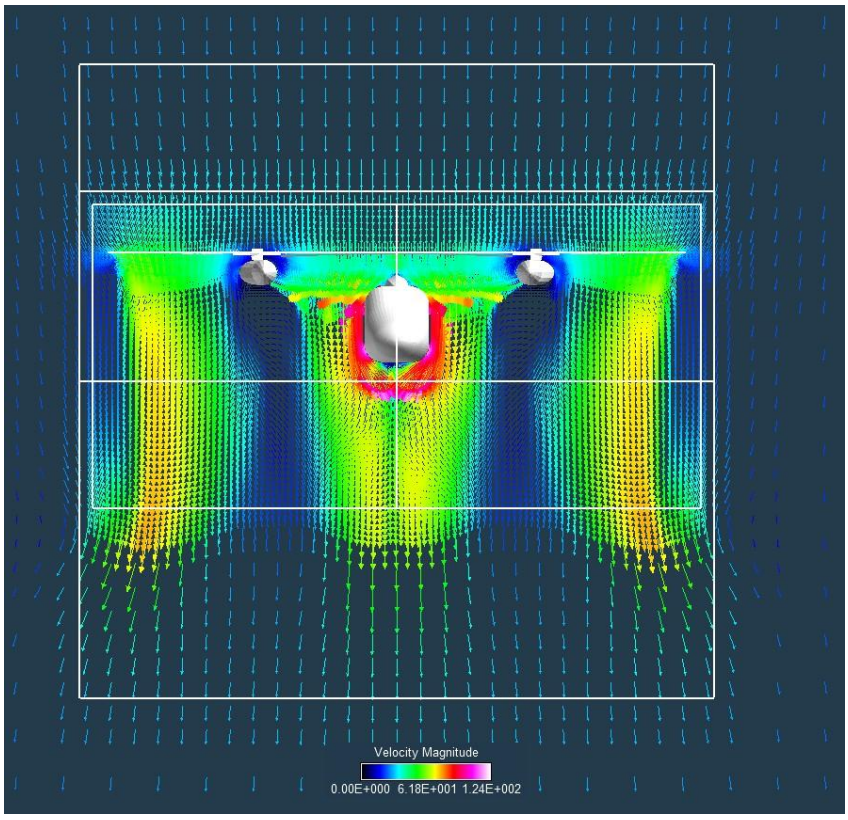

Case 24 (FF6 at 5000 feet):

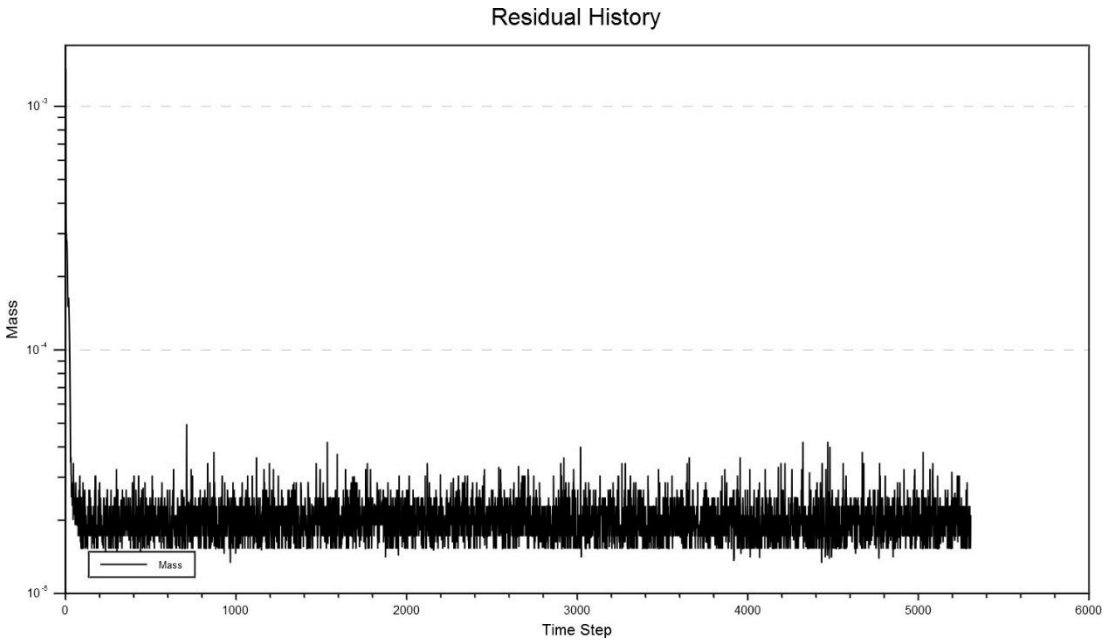

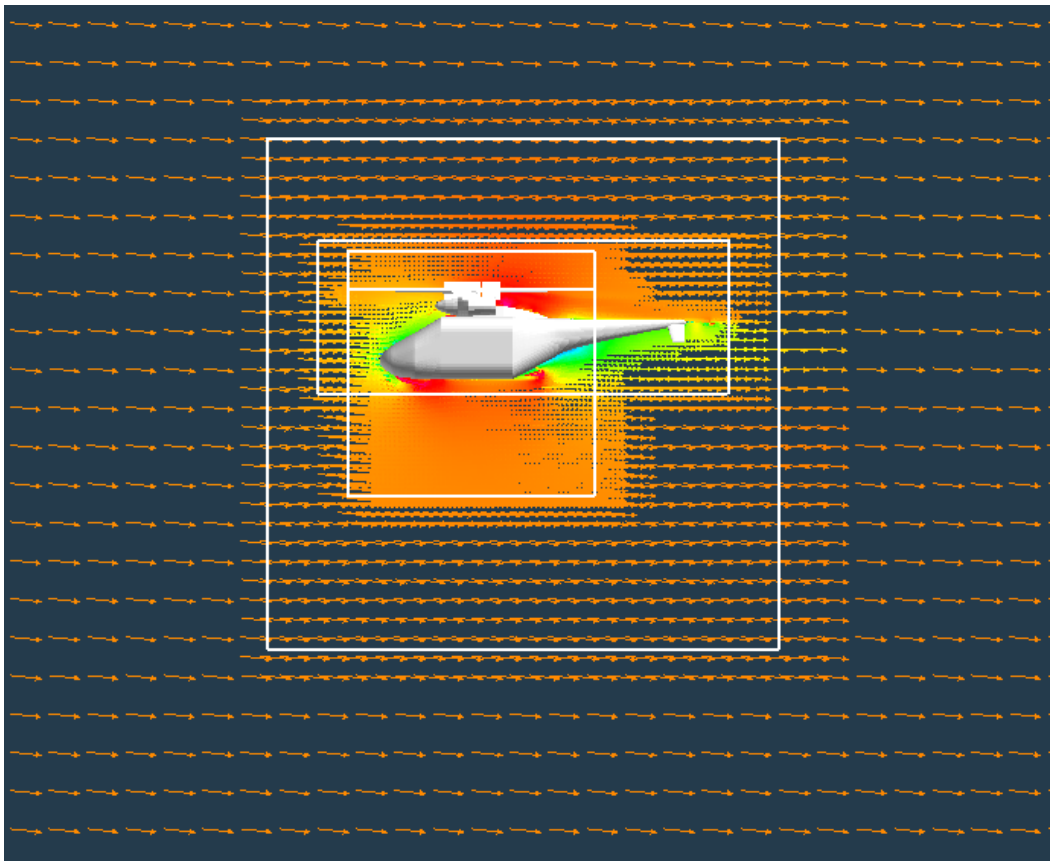

2. Unsuccessful Cases

Case 1:

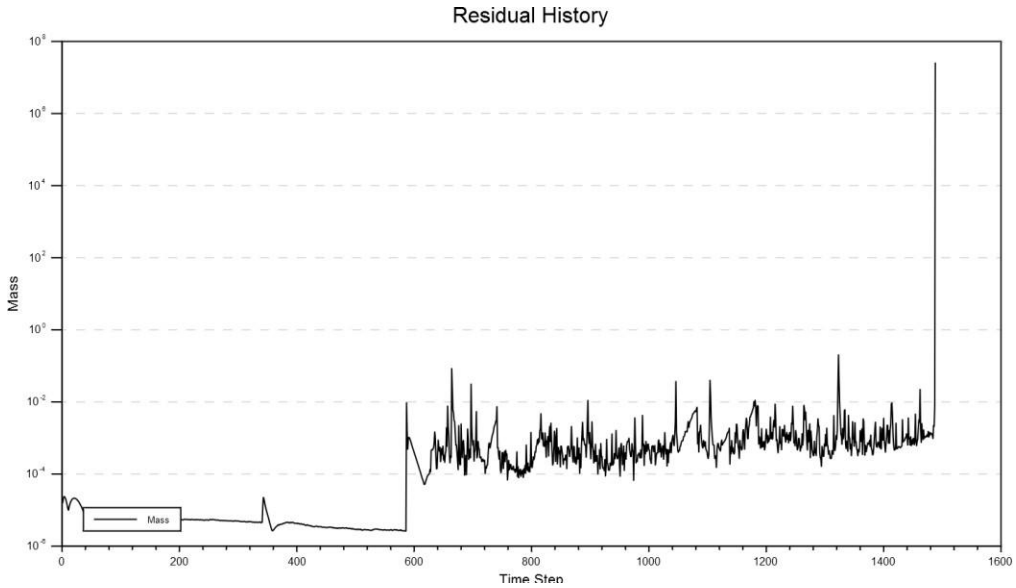

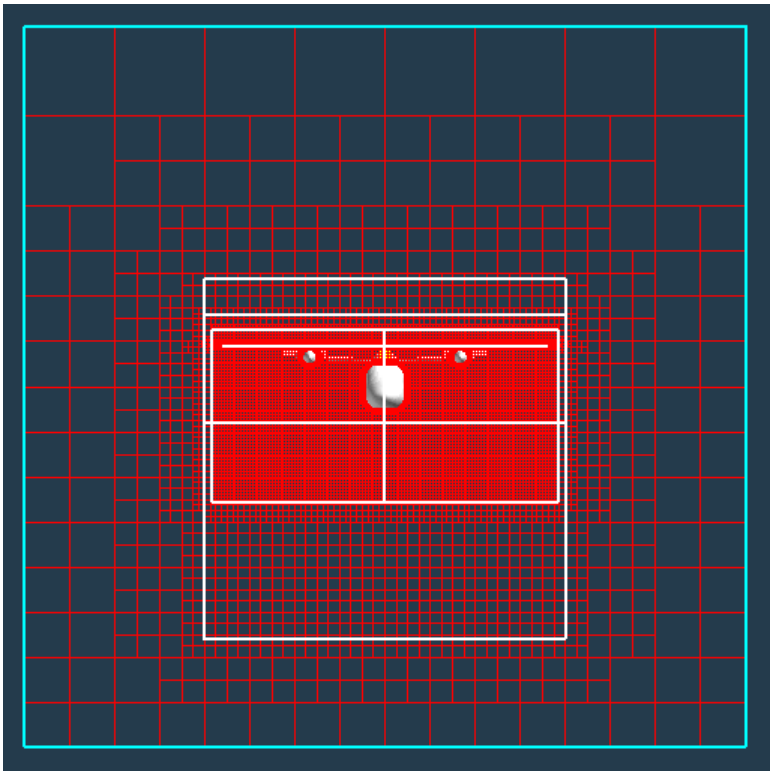

Failure reason: turbulence iteration diverged—low time grid.

Note: flow solution failed to load.

Case 2:

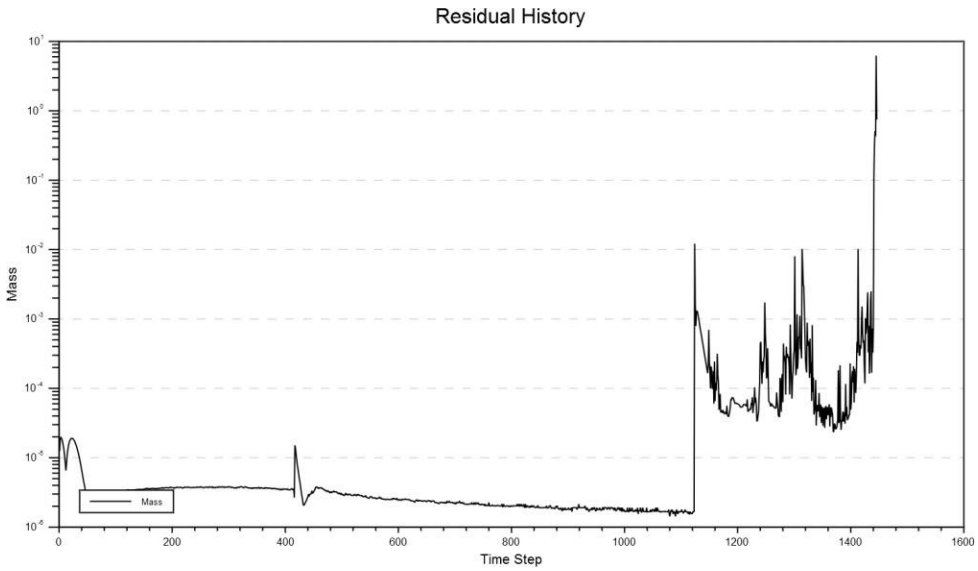

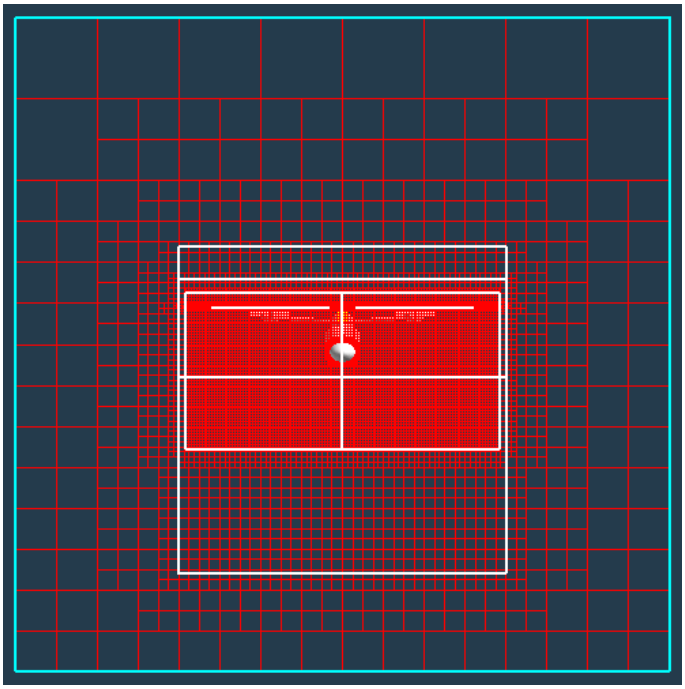

Failure reason: turbulence iteration diverged—coarse time grid.

Note: flow solution failed to load.

Case 3:

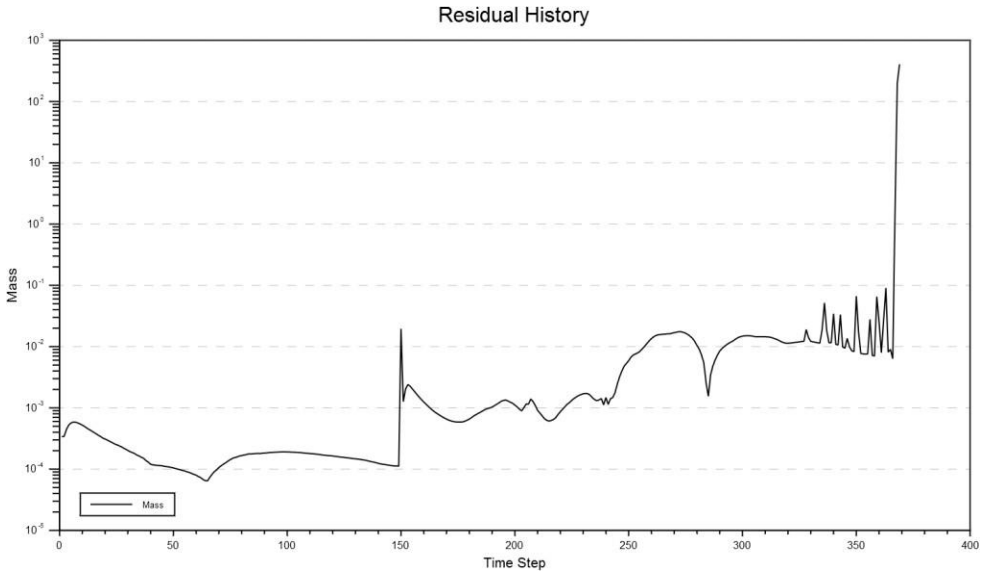

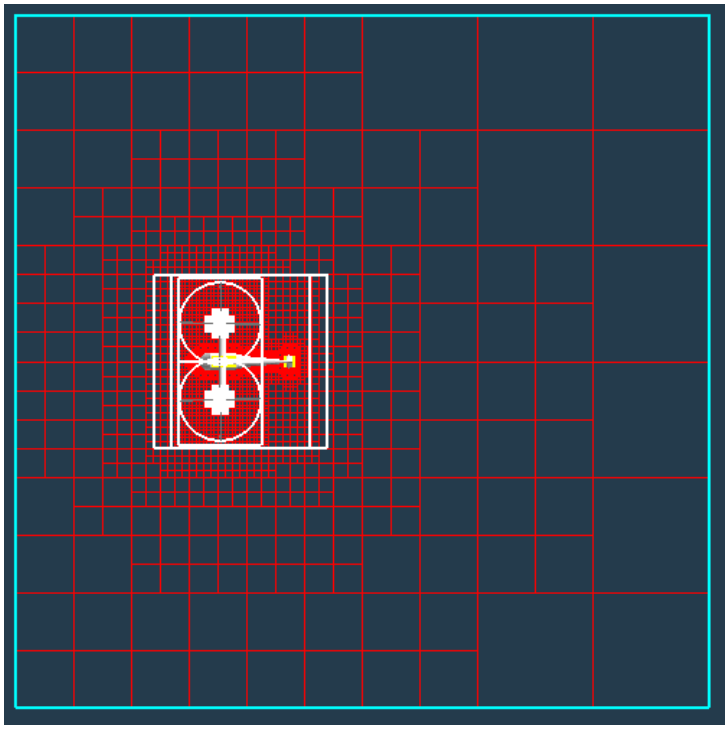

Failure reason: energy iteration diverged—result of 402.

Note: flow solution failed to load.

Case 4:

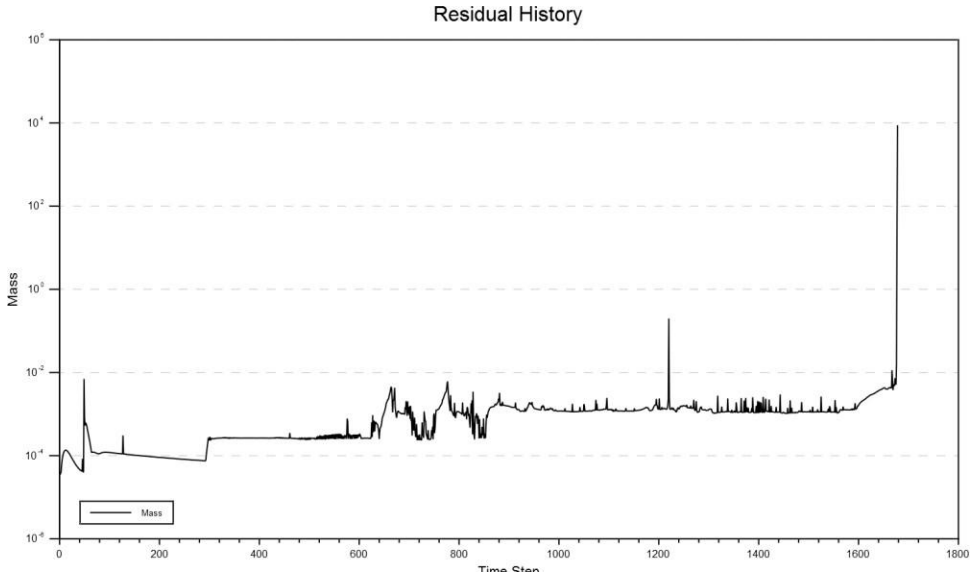

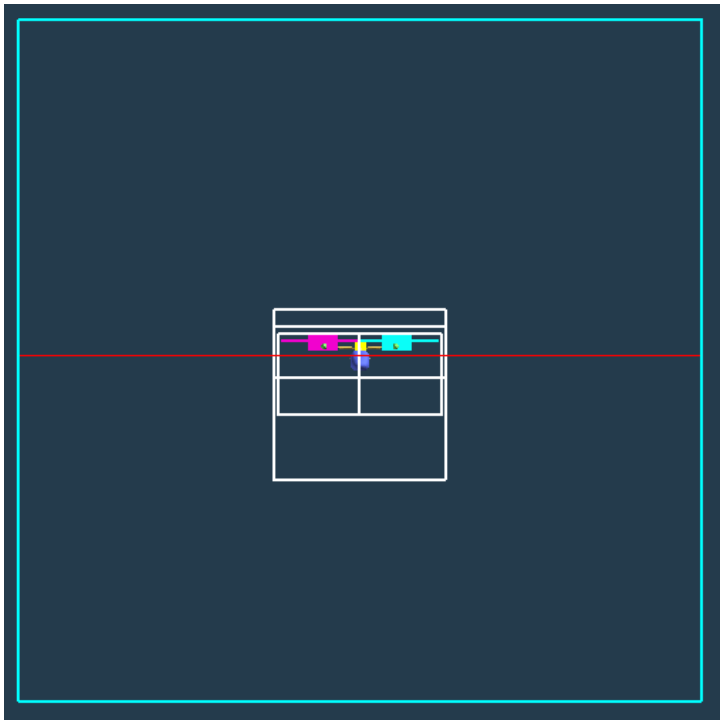

Failure reason: energy iteration diverged—result of 402.

Note: flow solution failed to load.

Case 5:

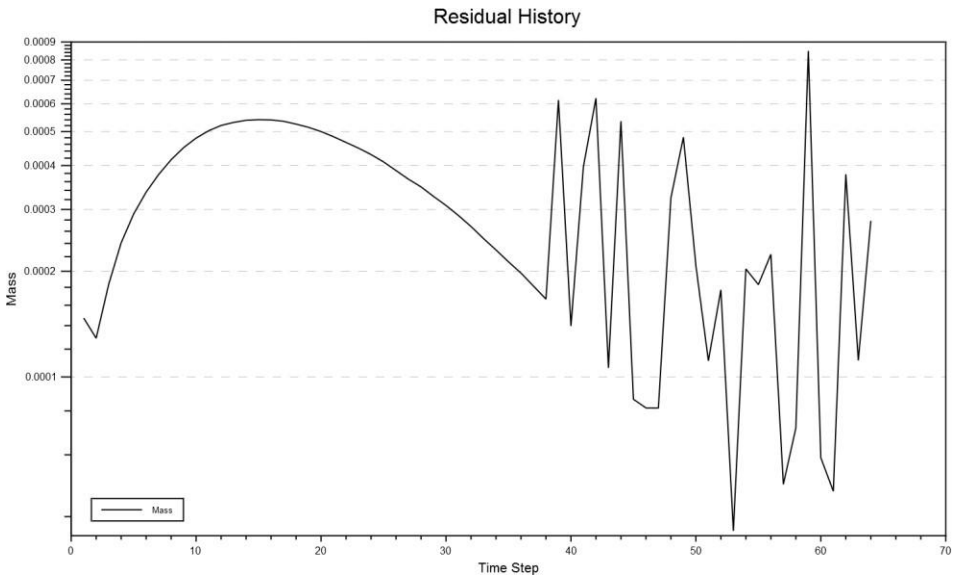

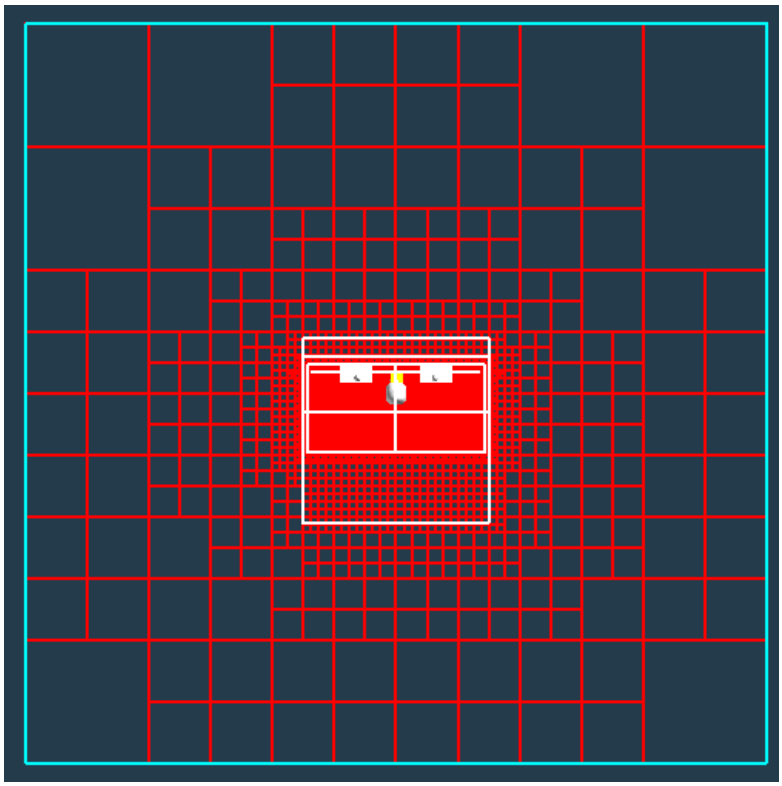

Failure Reason: energy iteration diverged—result of 402.

Note: flow solution failed to load.

Case 6:

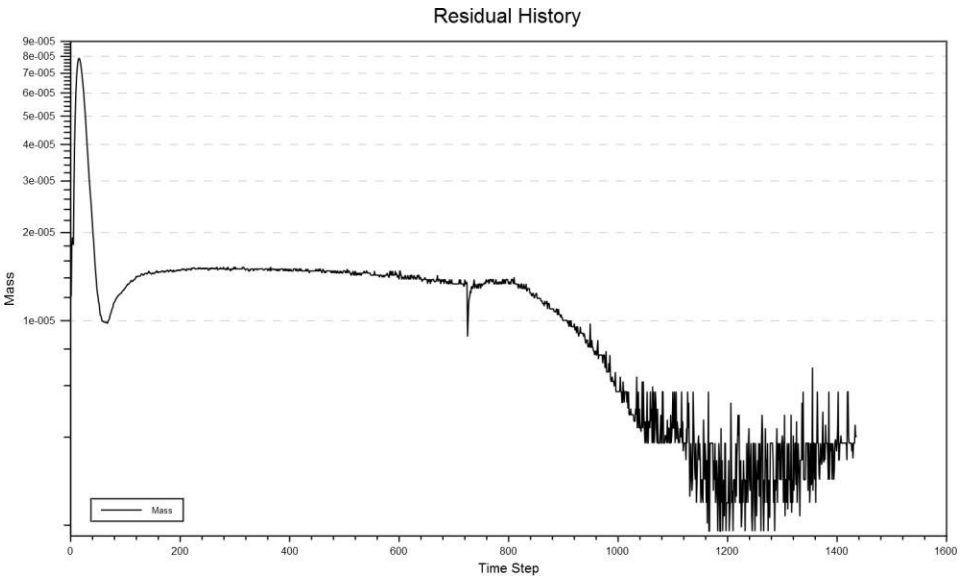

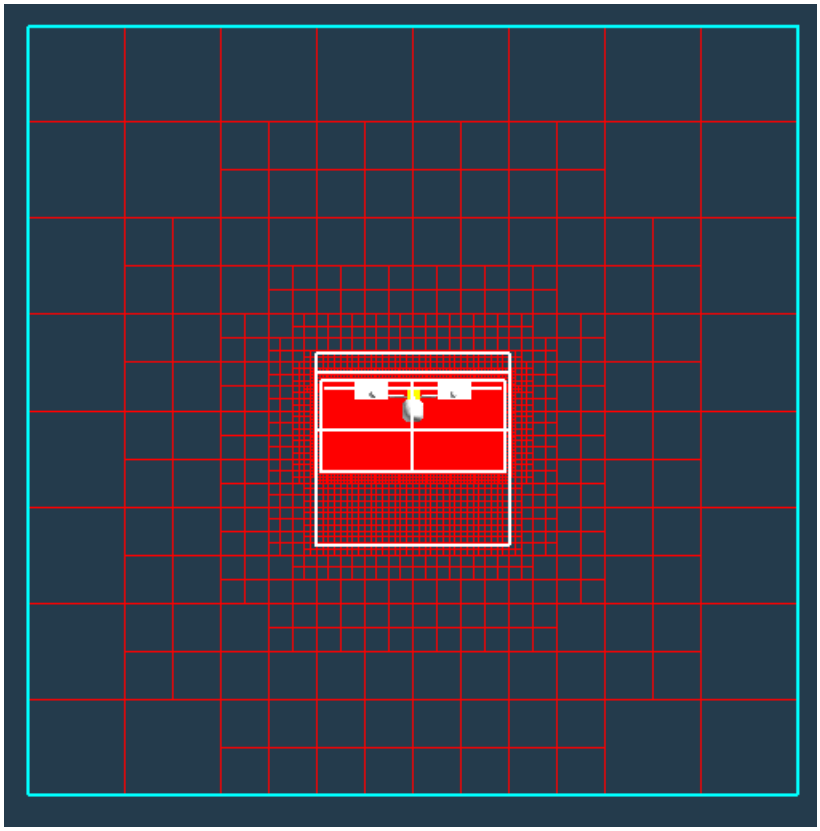

Failure reason: energy iteration diverged—result of 402.

Note: flow solution failed to load.

Case 7:

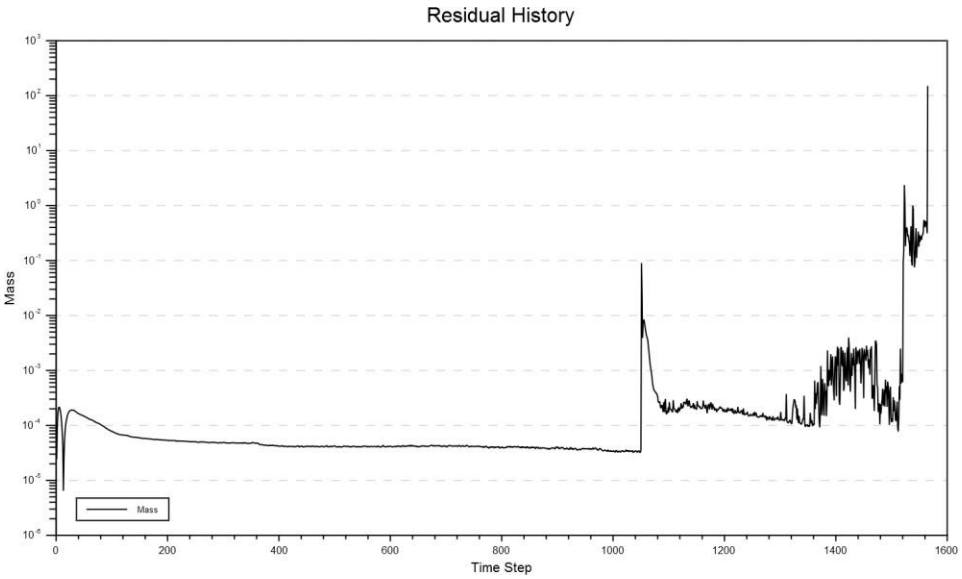

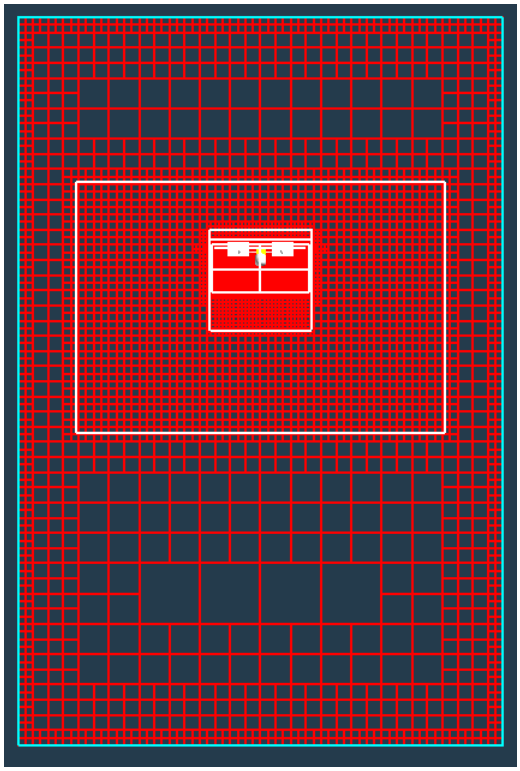

Failure reason: energy iteration diverged—result of 402.

Note: flow solution failed to load.

Case 8:

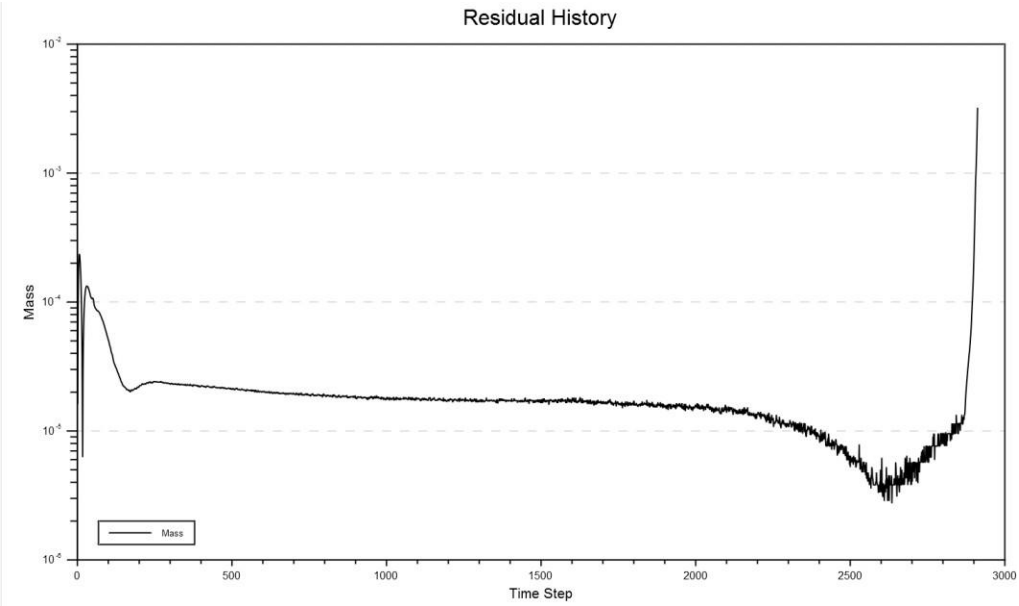

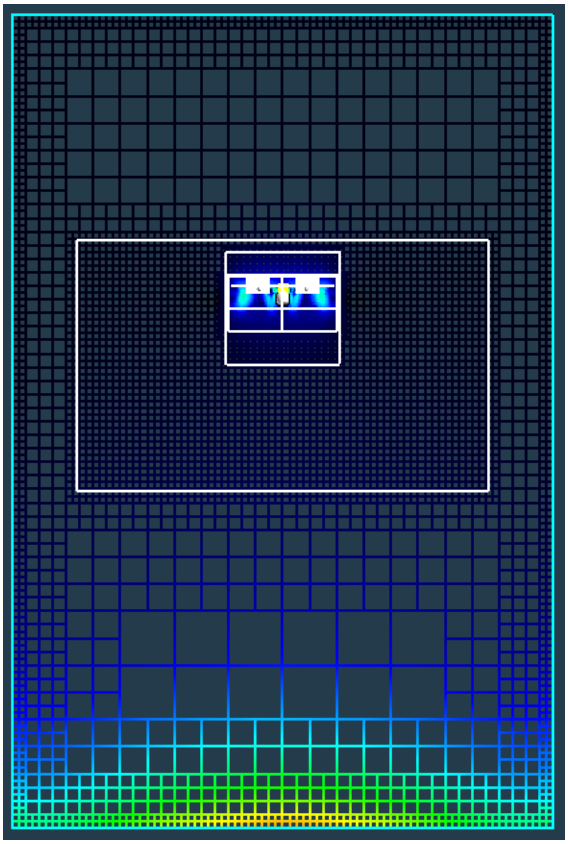

Failure reason: turbulence iteration diverged—coarse time grid.

Case 9:

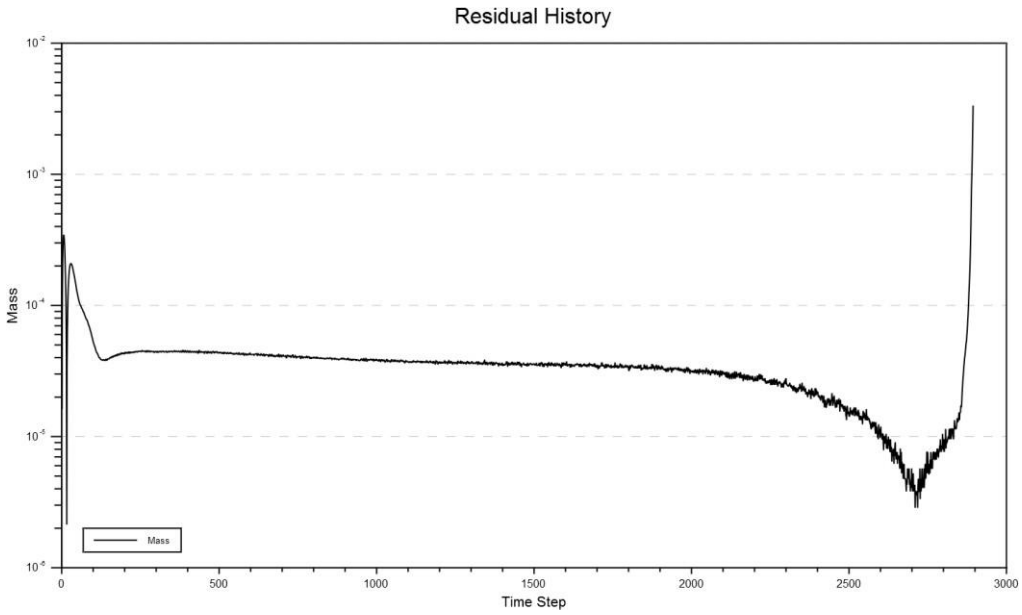

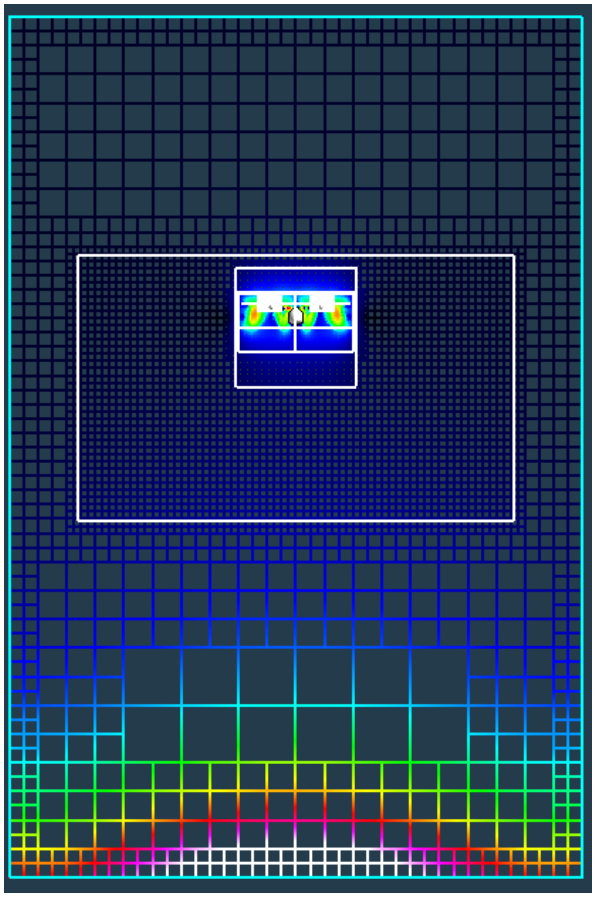

Failure reason: turbulence iteration diverged—coarse time grid.

Case 10:

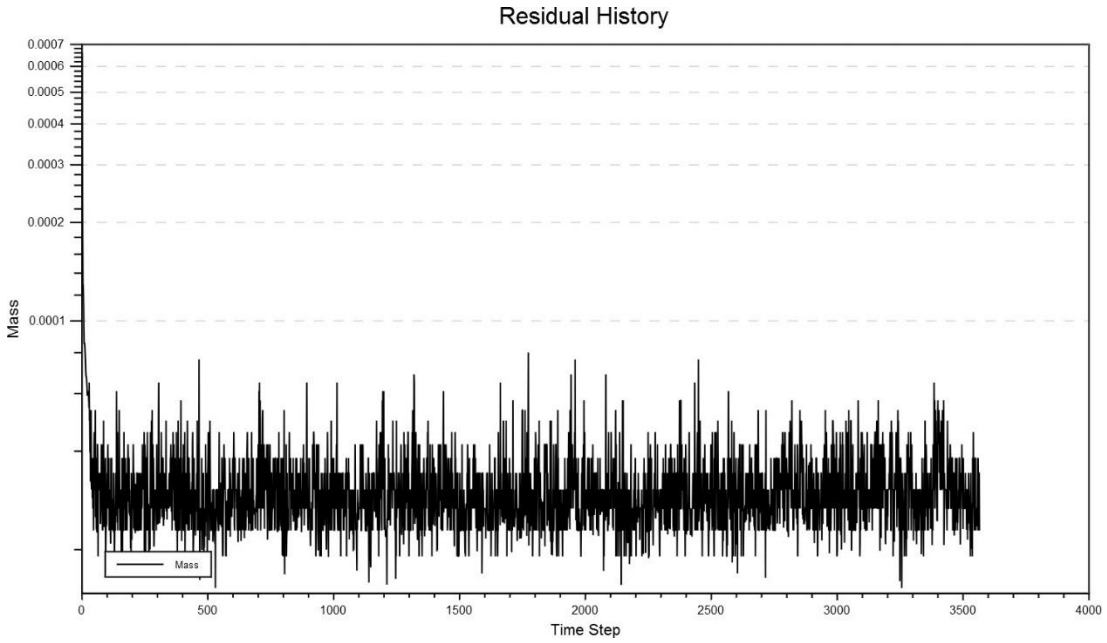

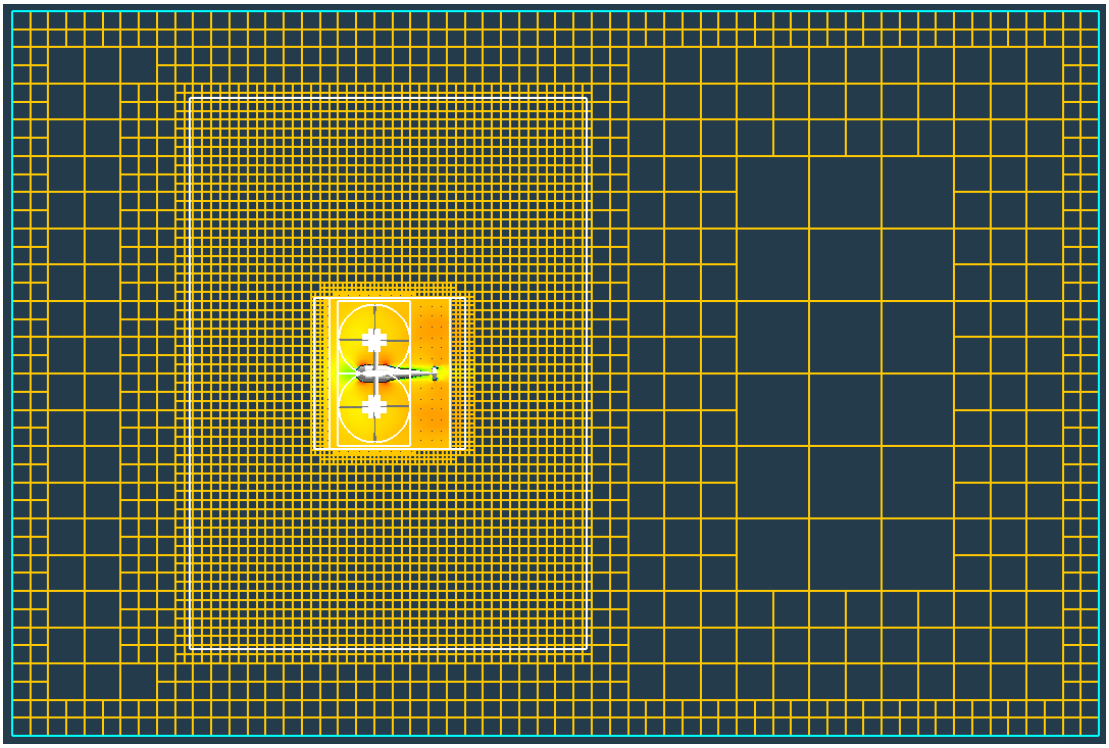

Failure reason: velocity below cruise speed.

Case 11:

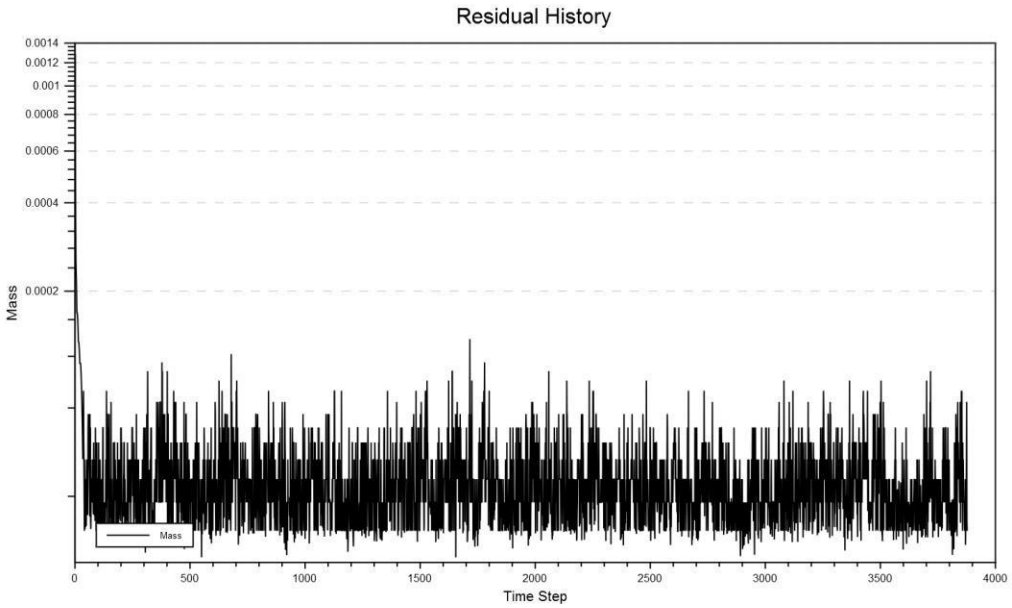

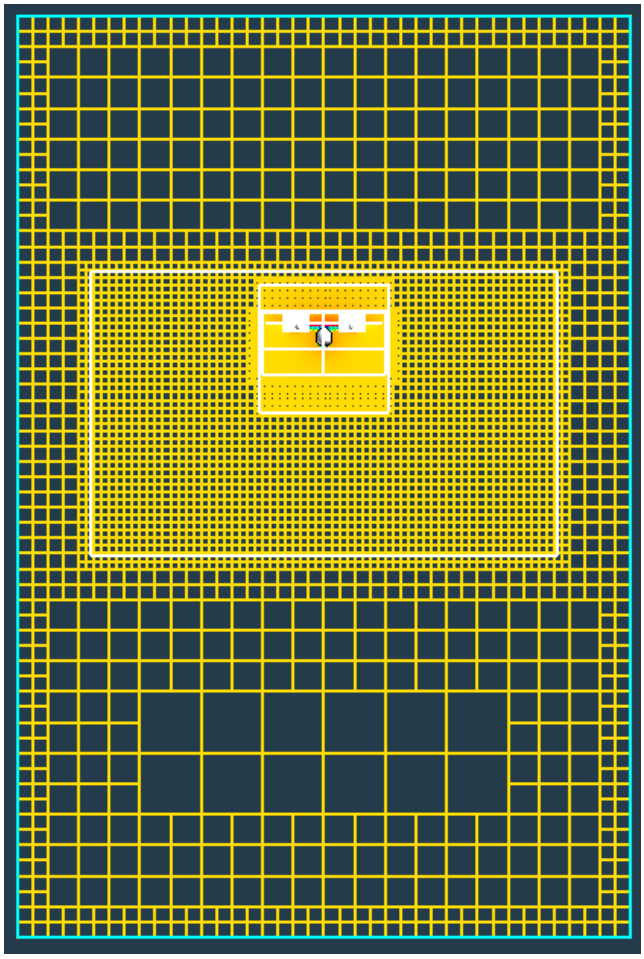

Failure reason: manually stopped before convergence.

Case 12:

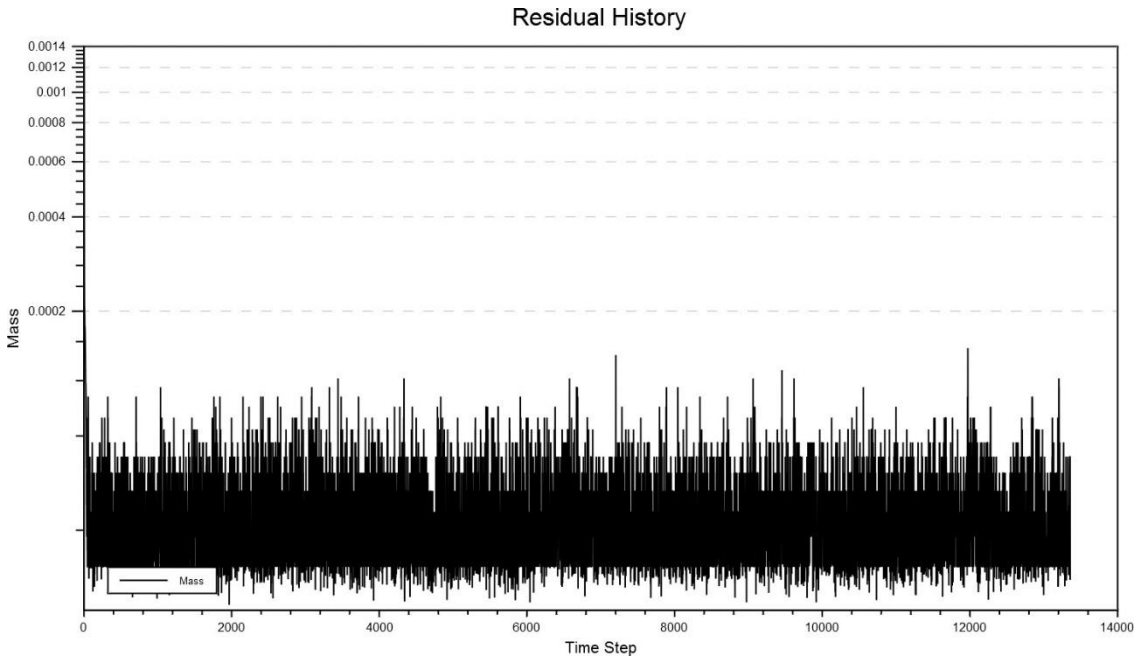

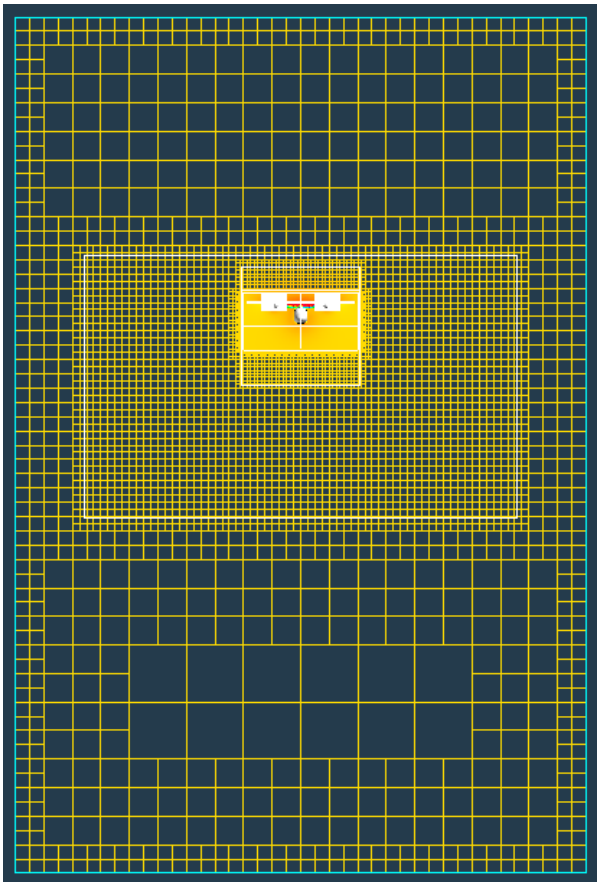

Failure reason: memory full, rotor performance unequal.

Case 13:

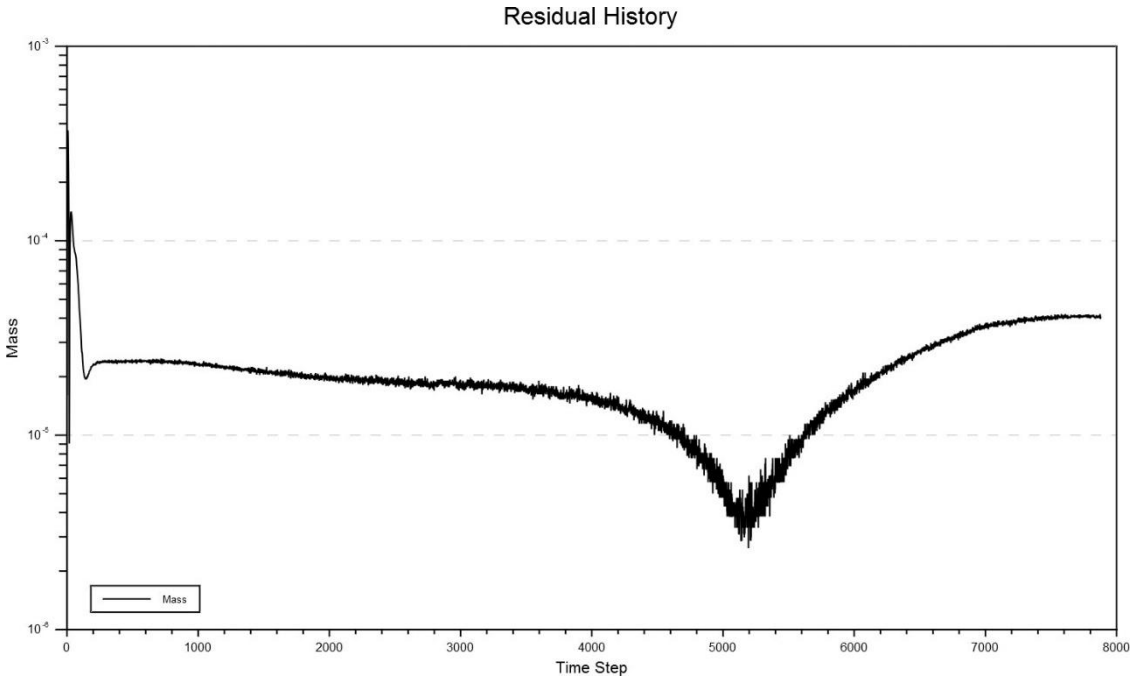

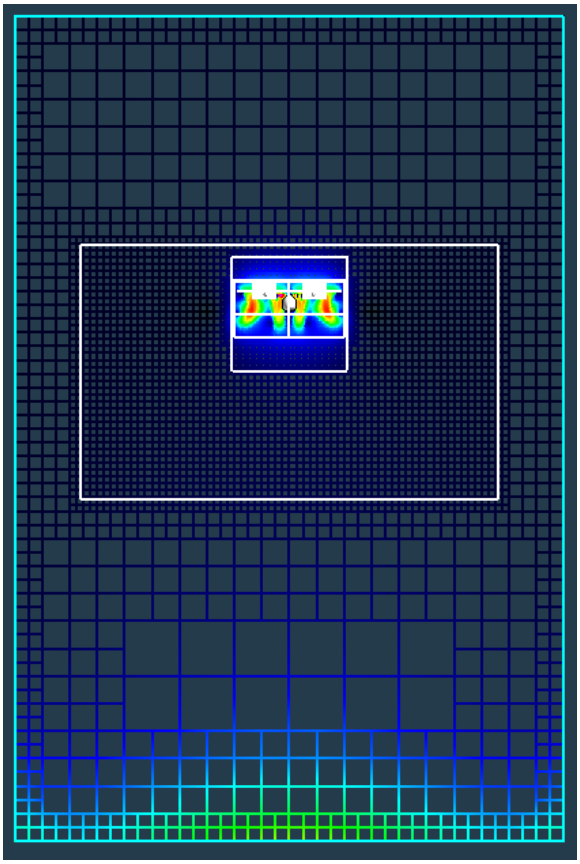

Failure reason: bad residuals.

Case 14:

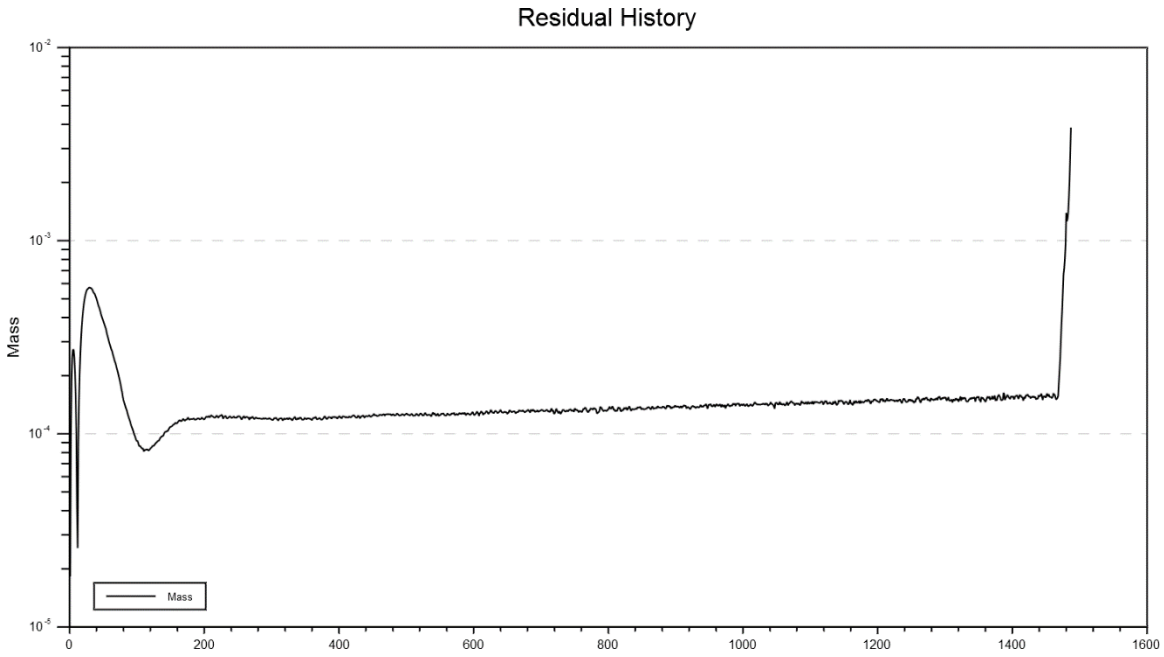

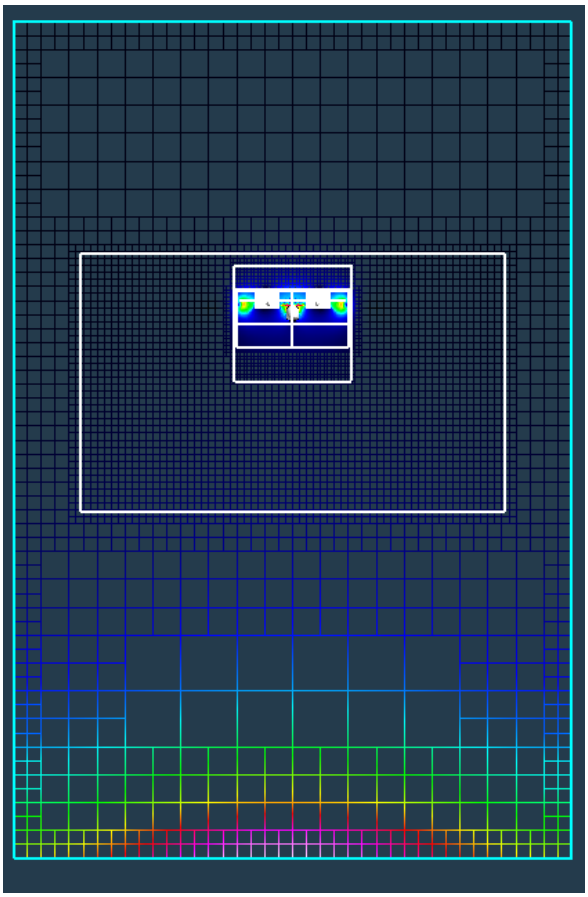

Failure reason: turbulence iteration diverged.

Case 16:

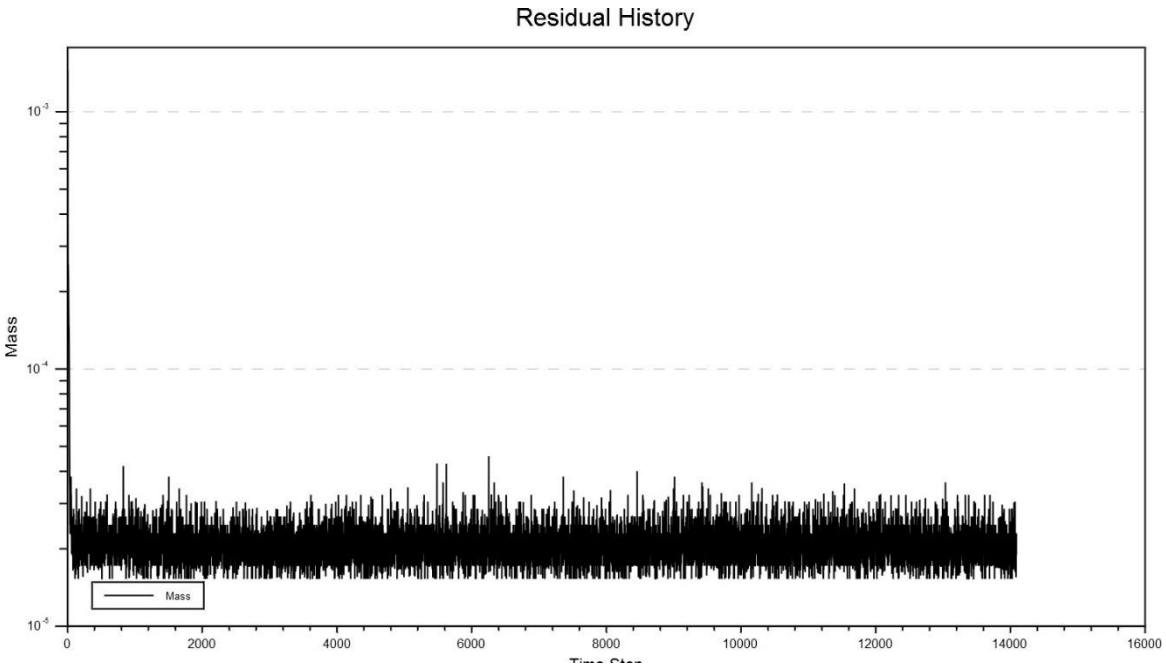

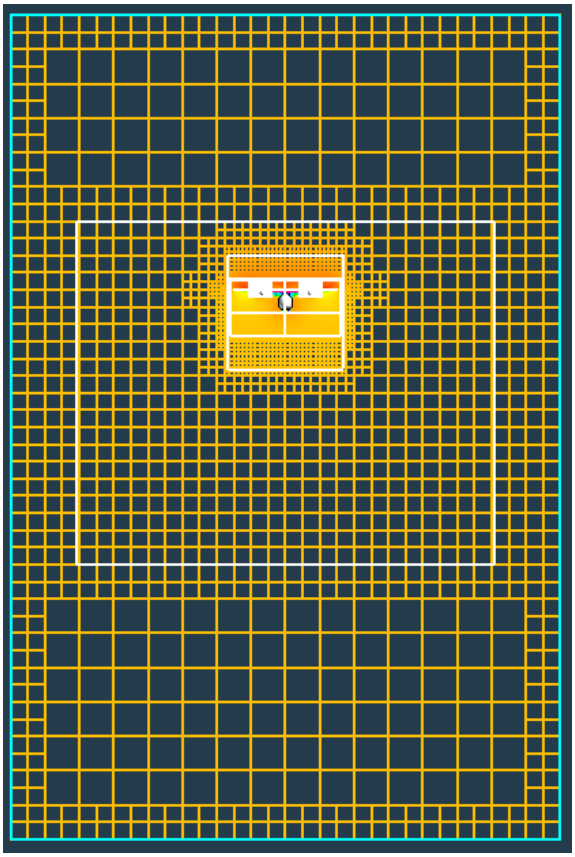

Failure reason: angle of attack input incorrectly.

Case 17:

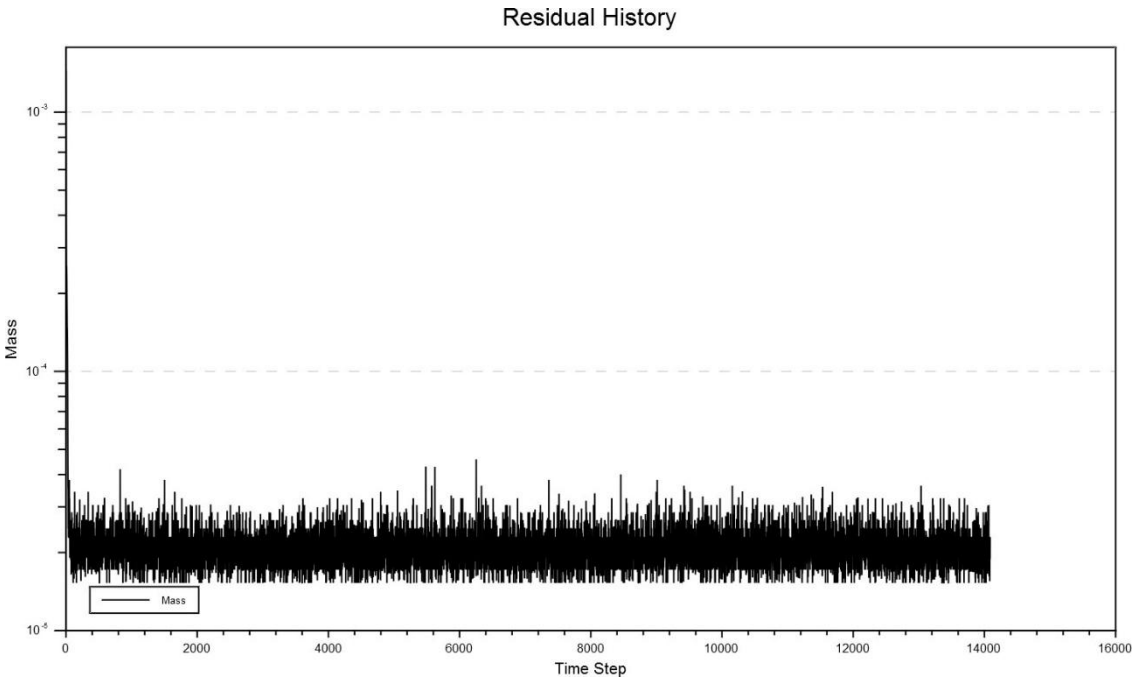

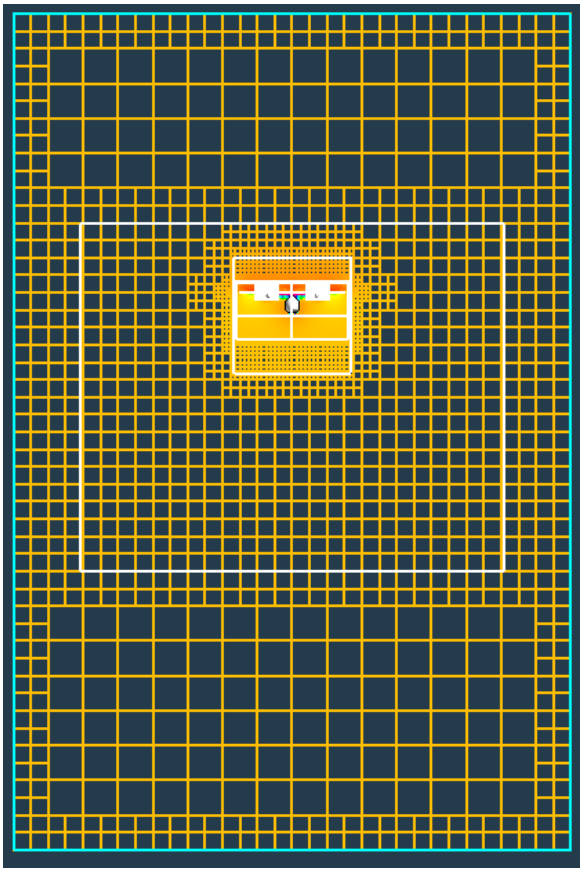

Failure reason: angle of attack input correctly.

Case 21:

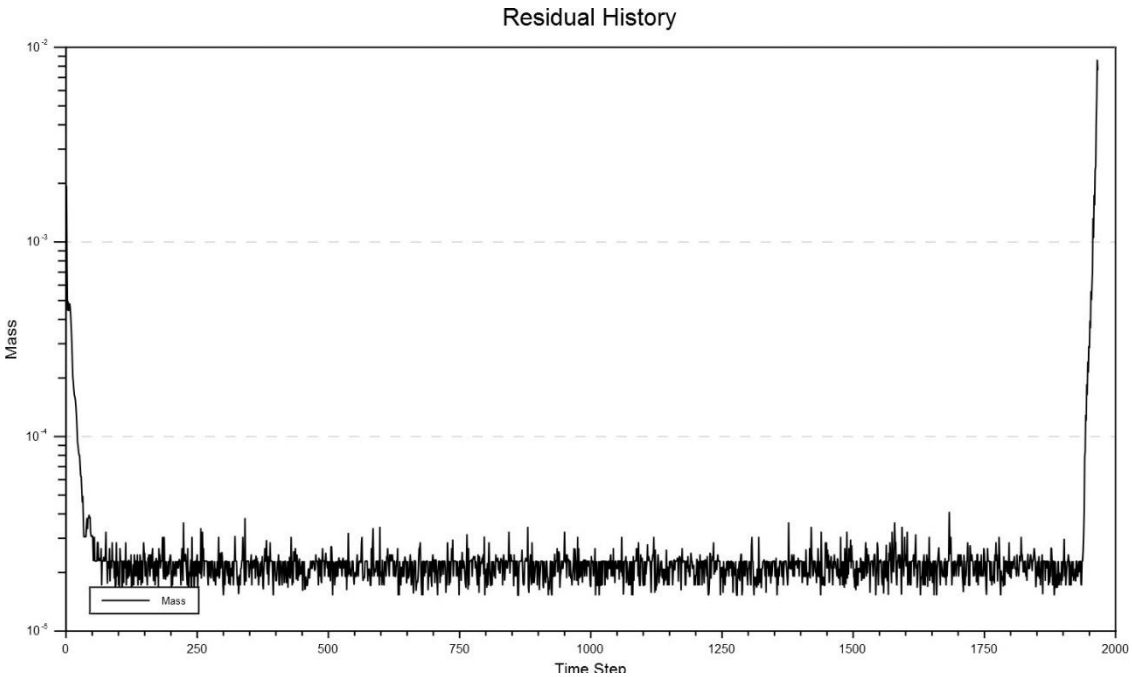

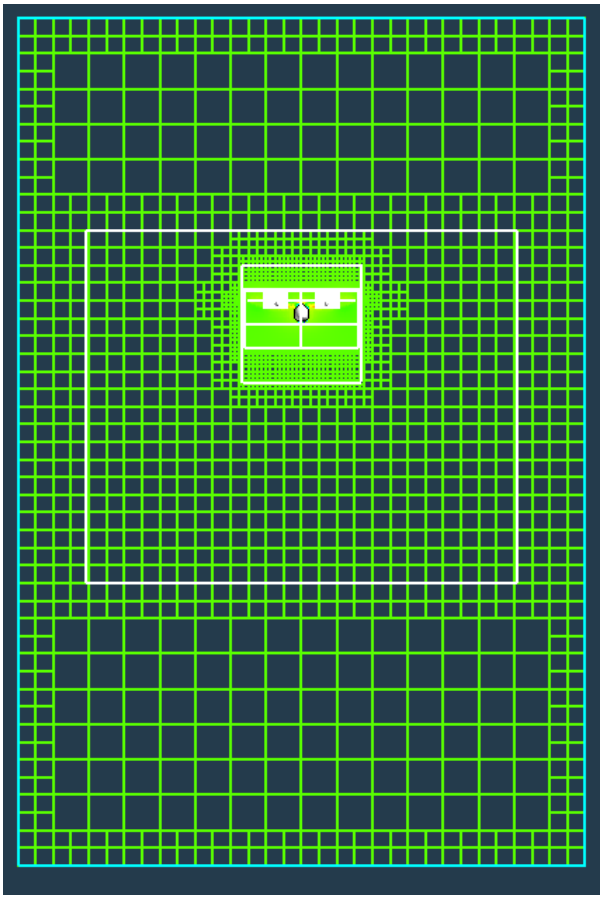

Failure reason: turbulence iteration diverged—stall point on rotors.

Case 22:

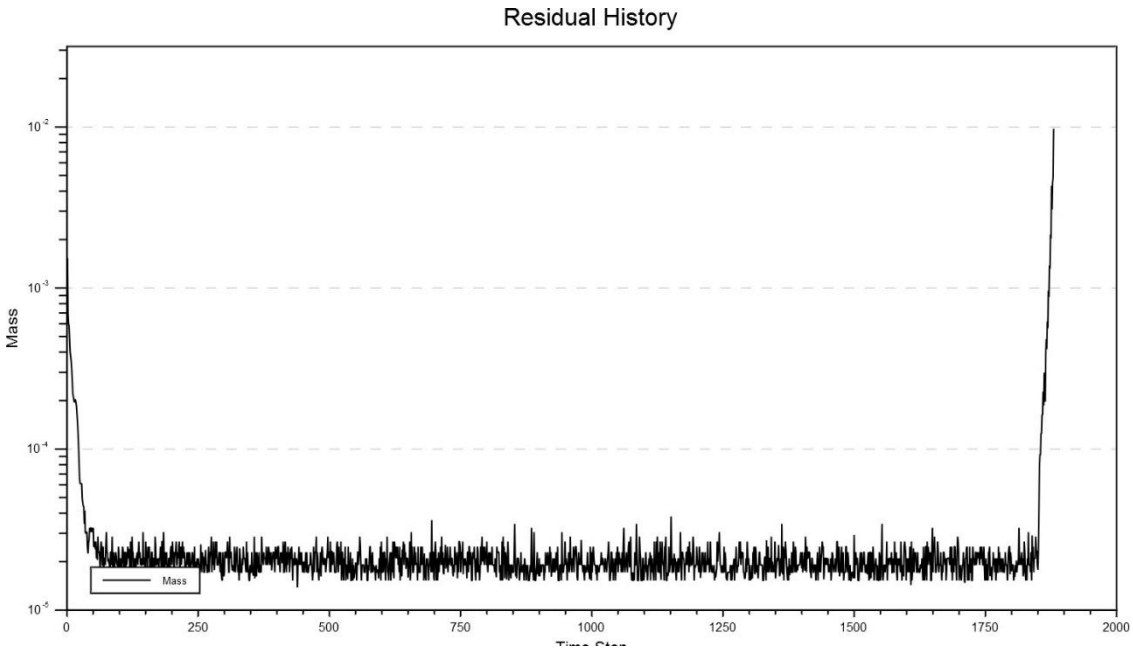

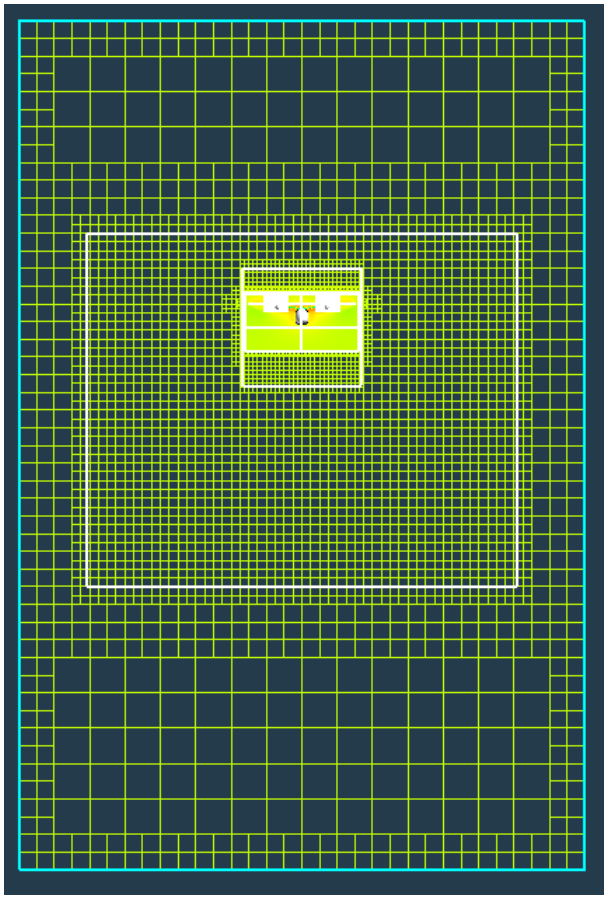

Failure reason: turbulence iteration diverged—stall point on rotors.